



HAL
open science

Design of Robust Radar Detectors Through Random Perturbation of the Target Signature

Angelo Coluccia, Giuseppe Ricci, Olivier Besson

► **To cite this version:**

Angelo Coluccia, Giuseppe Ricci, Olivier Besson. Design of Robust Radar Detectors Through Random Perturbation of the Target Signature. *IEEE Transactions on Signal Processing*, 2019, 67 (19), pp.5118-5129. 10.1109/TSP.2019.2935915 . hal-02641298

HAL Id: hal-02641298

<https://hal.science/hal-02641298>

Submitted on 28 May 2020

HAL is a multi-disciplinary open access archive for the deposit and dissemination of scientific research documents, whether they are published or not. The documents may come from teaching and research institutions in France or abroad, or from public or private research centers.

L'archive ouverte pluridisciplinaire **HAL**, est destinée au dépôt et à la diffusion de documents scientifiques de niveau recherche, publiés ou non, émanant des établissements d'enseignement et de recherche français ou étrangers, des laboratoires publics ou privés.



Open Archive Toulouse Archive Ouverte (OATAO)

OATAO is an open access repository that collects the work of some Toulouse researchers and makes it freely available over the web where possible.

This is an author's version published in: <https://oatao.univ-toulouse.fr/25980>

Official URL : <https://doi.org/10.1109/TSP.2019.2935915>

To cite this version :

Coluccia, Angelo and Ricci, Giuseppe and Besson, Olivier Design of Robust Radar Detectors Through Random Perturbation of the Target Signature. (2019) IEEE Transactions on Signal Processing, 67 (19). 5118-5129. ISSN 1053-587X

Any correspondence concerning this service should be sent to the repository administrator:

tech-oatao@listes-diff.inp-toulouse.fr

Design of Robust Radar Detectors Through Random Perturbation of the Target Signature

Angelo Coluccia , Senior Member, IEEE, Giuseppe Ricci , Senior Member, IEEE, and Olivier Besson 

Abstract—The paper addresses the problem of designing radar detectors more robust than Kelly’s detector to possible mismatches of the assumed target signature, but with no performance degradation under matched conditions. The idea is to model the received signal under the signal-plus-noise hypothesis by adding a random component, parameterized via a design covariance matrix, that makes the hypothesis more plausible in presence of mismatches. Moreover, an unknown power of such component, to be estimated from the observables, can lead to no performance loss, under matched conditions. Derivation of the (one-step) GLRT is provided for two choices of the design matrix, obtaining detectors with different complexity and behavior. A third parametric detector is also obtained by an ad-hoc generalization of one of such GLRTs. The analysis shows that the proposed approach can cover a range of different robustness levels that is not achievable by state-of-the-art with the same performance of Kelly’s detector under matched conditions.

Index Terms—Radar detection, adaptive signal detection, direction-of-arrival estimation, matched filter.

I. INTRODUCTION

A. Notation

VECTORS and matrices are denoted by boldface lower-case and upper-case letters, respectively. The symbols $|\cdot|$, $\|\cdot\|$, $\det(\cdot)$, $\text{tr}(\cdot)$, T , † , denote modulus value, Euclidean norm, determinant, trace, transpose, and conjugate transpose (Hermitian), respectively. $E[\cdot]$ is the statistical expectation operator. \mathbb{C} is the set of complex numbers and $\mathbb{C}^{N \times M}$ is the Euclidean space of $(N \times M)$ -dimensional complex matrices. $\mathbf{0}$ is the null vector of proper dimension and \mathbf{I}_N stands for the $N \times N$ identity matrix. \mathbf{P}_u^\perp is the (orthogonal) projection matrix onto the orthogonal complement of the subspace spanned by the vector \mathbf{u} . Finally, we write $\mathbf{x} \sim \mathcal{CN}_N(\mathbf{0}, \mathbf{M})$ if \mathbf{x} is an N -dimensional complex normal vector with zero mean and (Hermitian) positive definite covariance matrix \mathbf{M} .

B. Existing Results and Motivation

The well-known problem of detecting the possible presence of a coherent return from a given cell under test (CUT) in range,

doppler, and azimuth, is classically formulated as the following hypothesis testing problem:

$$\begin{cases} H_0 : & \mathbf{z} = \mathbf{n} \\ H_1 : & \mathbf{z} = \alpha \mathbf{v} + \mathbf{n} \end{cases} \quad (1)$$

where $\mathbf{z} \in \mathbb{C}^{N \times 1}$, $\mathbf{n} \in \mathbb{C}^{N \times 1}$, and $\mathbf{v} \in \mathbb{C}^{N \times 1}$ are the received vector, corresponding noise term, and known space-time steering vector of the useful target echo. In general N is the number of processed samples from the CUT; it might be the number of antenna array elements times the number of pulses [1], [2]. The noise term is often modeled according to the complex normal distribution with zero mean and unknown (Hermitian) positive definite covariance matrix \mathbf{C} , i.e., $\mathbf{n} \sim \mathcal{CN}_N(\mathbf{0}, \mathbf{C})$. Modeling $\alpha \in \mathbb{C}$ as an unknown deterministic parameter returns a complex normal distribution for \mathbf{z} under both hypotheses; the non-zero mean under H_1 makes it possible to discriminate the two hypotheses

$$\begin{cases} H_0 : & \mathbf{z} \sim \mathcal{CN}_N(\mathbf{0}, \mathbf{C}) \\ H_1 : & \mathbf{z} \sim \mathcal{CN}_N(\alpha \mathbf{v}, \mathbf{C}). \end{cases} \quad (2)$$

In the pioneering paper by Kelly [3], the generalized likelihood ratio test (GLRT) is derived for (2), assuming a set of $K \geq N$ independent and identically distributed training (or secondary) data $\mathbf{r}_1, \dots, \mathbf{r}_K$, independent also of \mathbf{z} , free of target echoes, and sharing with the CUT the statistical characteristics of the noise, is available. In [4] the performance of such a detector is assessed when the actual steering vector is not aligned with the nominal one. The analysis shows that it is a selective receiver, i.e., it may have excellent rejection capabilities of signals arriving from directions different from the nominal one. A selective detector is desirable for target localization. Instead, when a radar is working in searching mode, a certain level of robustness to mismatches is preferable. For this reason, many works have addressed the problem of enhancing either the selectivity or the robustness of radar detectors to mismatches. In particular, the adaptive matched filter (AMF) [5], which solves (2) following a two-step approach, is a prominent example of robust detector, while the adaptive coherence estimator (ACE, also known as adaptive normalized matched filter) [6] is another example of selective receiver. Other relevant examples of selective receivers are obtained by solving a modified hypothesis testing problem that assumes the presence of a (fictitious) coherent signal under the noise-only (H_0) hypothesis to make it more plausible in presence of signal mismatches [7]–[9]. A family of receivers, obtained by inserting a nonnegative parameter in the original Kelly’s detector, has been proposed by Kalson in [10]; such a parameter, indicated as β in the following, allows one to control the degree to which mismatched signals are rejected, so

The associate editor coordinating the review of this manuscript and approving it for publication was Dr. Xavier Mestre. (Corresponding author: Angelo Coluccia.)

A. Coluccia and G. Ricci are with the Dipartimento di Ingegneria dell’Innovazione, Università del Salento, 73100 Lecce, Italy (e-mail: angelo.coluccia@unisalento.it; giuseppe.ricci@unisalento.it).

O. Besson is with ISAE-SUPAERO, 31055 Toulouse, France (e-mail: olivier.besson@isae-supaero.fr).

Digital Object Identifier 10.1109/TSP.2019.2935915

obtaining behaviors in between the AMF and Kelly’s detector. A different tunable receiver called KWA has been proposed in [11], which encompasses as special cases Kelly’s and W-ABORT detectors [9]. Although designed for enhanced selectivity, for values of its tunable parameter γ smaller than 1/2 it behaves as a robust detector, reaching the energy detector for $\gamma = 0$. Tunable receivers have also been proposed in [12], [13]. Other approaches, as for instance those based on the cone idea, can guarantee an increased robustness at the price of a certain loss under matched conditions [14], [15]. A robust two-stage detector obtained by cascading a GLRT-based subspace detector and the Rao test has been proposed in [16]. Robust and selective detectors have also been considered in the context of subspace detection [17]–[19]. Multidimensional/multichannel signal detection in homogeneous or partially homogeneous Gaussian disturbance (with unknown covariance matrix and unknown structured deterministic interference) is considered in [20], [21].

On the other hand, modeling $\alpha \in \mathbb{C}$ as a complex normal random variable with zero mean and variance $\overline{|\alpha|^2} = E[|\alpha|^2]$, returns a zero-mean complex normal distribution for z under both hypotheses; hence

$$\begin{cases} H_0 : z \sim \mathcal{CN}_N(\mathbf{0}, \mathbf{C}) \\ H_1 : z \sim \mathcal{CN}_N(\mathbf{0}, \mathbf{C} + \overline{|\alpha|^2} \mathbf{v} \mathbf{v}^\dagger). \end{cases} \quad (3)$$

This is a “second-order” approach to target modeling, i.e., the presence of a useful signal (H_1 hypothesis) is modeled in terms of a modification of the noise covariance matrix, instead of appearing in the mean as conversely for the more classical problem (2). Interesting properties in terms of either rejection capabilities or robustness to mismatches on the nominal steering vector can be obtained by considering a random (instead of deterministic) target signal, depending on the way problem (3) is solved and possibly on the presence of a fictitious signal under H_0 [22], [23].

In this paper, we investigate the potential of a detector that solves the following new hypothesis testing problem

$$\begin{cases} H_0 : z = \mathbf{n} \\ H_1 : z = \alpha \mathbf{v} + \boldsymbol{\theta} + \mathbf{n} \end{cases} \quad (4)$$

where α is an unknown deterministic parameter and $\boldsymbol{\theta} \sim \mathcal{CN}_N(\mathbf{0}, \nu \boldsymbol{\Sigma})$ represents a random component. The goal is to obtain a detector that exhibits the same probability of detection (P_d) of Kelly’s GLRT under matched conditions, but is more robust than the latter to mismatches between the nominal steering vector and the actual one. In the existing literature, the “win-win” situation in which robustness is achieved without any loss under matched conditions has been obtained so far through careful parameter setting of tunable receivers, notably the mentioned Kalson’s and KWA detectors; here we propose a different approach which, remarkably, can cover levels of robustness that are not possible with such state-of-the-art receivers. The idea in (4) is in fact to add to the H_1 hypothesis a signal $\boldsymbol{\theta}$ that makes H_1 more plausible, hence hopefully the detector more robust to mismatches on the nominal steering vector \mathbf{v} . To this aim, a design matrix $\boldsymbol{\Sigma}$ is considered, multiplied by an unknown factor ν ; in doing so, in case of matched signature no component will be likely found along $\boldsymbol{\Sigma}$ and the conventional case is recovered, i.e., the estimated value for ν will be likely zero; conversely, if

the mismatch causes some leakage of the signal that is captured by $\boldsymbol{\Sigma}$, the detector would tend to decide for H_1 more likely.

If we suppose that $\boldsymbol{\theta}$ is independent of \mathbf{n} , the resulting hypothesis testing problem turns out to be

$$\begin{cases} H_0 : z \sim \mathcal{CN}_N(\mathbf{0}, \mathbf{C}) \\ H_1 : z \sim \mathcal{CN}_N(\alpha \mathbf{v}, \mathbf{C} + \nu \boldsymbol{\Sigma}). \end{cases} \quad (5)$$

In summary, the contribution of this paper is threefold:

- A new hypothesis test (5) for radar detection is introduced, which is a possible generalization of (2) and (3).
- The (one-step) GLRT is derived for two choices of the design matrix $\boldsymbol{\Sigma}$. A third parametric detector is obtained by an ad-hoc generalization of one of such GLRTs. Two-step GLRT-based detectors have been presented in our preliminary work [24]. The detectors derived here have different complexity and behavior.
- A thorough analysis of the proposed detectors is performed, also deriving closed-form expressions for the P_{fa} for two of the detectors and showing that they have the desirable constant false alarm rate (CFAR) property. The performance assessment reveals that the proposed approach can guarantee negligible loss under matched conditions with respect to Kelly’s detector while providing diversified degrees of robustness depending on chosen parameters.

The paper is organized as follows: Section II is devoted to the derivation of the GLRTs (with some proofs and lengthy manipulations in the Appendices). Section III addresses the analysis of the detectors. We conclude in Section IV.

II. GLRTS FOR POINT-LIKE TARGETS

In this section, we derive robust detectors employing the GLRT. To this end, we consider the following binary hypothesis testing problem

$$\begin{cases} H_0 : z \sim \mathcal{CN}_N(\mathbf{0}, \mathbf{C}) \\ \quad \mathbf{r}_k \sim \mathcal{CN}_N(\mathbf{0}, \mathbf{C}), \quad k = 1, \dots, K \\ H_1 : z \sim \mathcal{CN}_N(\alpha \mathbf{v}, \nu \boldsymbol{\Sigma} + \mathbf{C}) \\ \quad \mathbf{r}_k \sim \mathcal{CN}_N(\mathbf{0}, \mathbf{C}), \quad k = 1, \dots, K \end{cases}$$

where we recall that the training data \mathbf{r}_k form a set of $K \geq N$ independent (and identically distributed) vectors,¹ independent also of z , free of target echoes, and sharing with the CUT the statistical characteristics of the noise. The positive definite matrix \mathbf{C} , $\nu \geq 0$, and $\alpha \in \mathbb{C}$ are unknown quantities while $\mathbf{v} \in \mathbb{C}^{N \times 1}$ is a known vector. As to the (Hermitian) positive semidefinite matrix $\boldsymbol{\Sigma}$, it might be either known or unknown. In the former case, $\boldsymbol{\Sigma}$ reflects our knowledge about the random variations of the target steering vector around its nominal value \mathbf{v} . On the contrary, an unknown $\boldsymbol{\Sigma}$ implies that no specific knowledge is available. In such a case, obviously $\boldsymbol{\Sigma}$ cannot be estimated from a single snapshot (data from the CUT) and therefore one needs to make some further assumptions. The latter are mostly dictated by pragmatism so that the detection problem remains identifiable and mathematically tractable. Indeed, $\boldsymbol{\Sigma}$ should be viewed as a means to model the structure of the variations around \mathbf{v} while ν captures their amplitudes. In any case, one has to look

¹The condition $K \geq N$ ensures that the sample covariance matrix based on training data has full rank with probability one [3].

at the ultimate performance for judging the goodness of each choice. In the sequel, we will assume that either Σ is a known rank-one matrix or $\Sigma = \mathbf{C}$ (so that, although unknown, it does not introduce new unknowns).

A. Case 1: Derivation of the GLRT for $\Sigma = \mathbf{u}\mathbf{u}^\dagger$

In this section, we address the case that Σ is a rank-one matrix. First observe that *the case $\Sigma = \mathbf{v}\mathbf{v}^\dagger$, which enforces the target signature in both the mean and covariance,² returns Kelly's detector*, as discussed later in this section. We are instead more interested in a vector \mathbf{u} aimed at making the H_1 hypothesis more plausible under mismatches. Intuitively, a design matrix $\Sigma = \mathbf{v}_m\mathbf{v}_m^\dagger$, where \mathbf{v}_m is a slightly mismatched steering vector, is a possible way to introduce some robustness without appreciable loss under matched conditions; nonetheless, other choices are possible, hence we provide a derivation for generic $\Sigma = \mathbf{u}\mathbf{u}^\dagger$.

The corresponding GLRT is given by

$$\Lambda(\mathbf{z}, \mathbf{S}) = \frac{\max_{\mathbf{C} > 0} \max_{\nu \geq 0} \max_{\alpha \in \mathbb{C}} f_1(\mathbf{z}, \mathbf{S} | \mathbf{C}, \nu, \alpha)}{\max_{\mathbf{C} > 0} f_0(\mathbf{z}, \mathbf{S} | \mathbf{C})} \underset{H_0}{\overset{H_1}{\leq}} \eta \quad (6)$$

where

$$f_1(\mathbf{z}, \mathbf{S} | \mathbf{C}, \nu, \alpha) = \frac{e^{-\text{tr}[(\nu \mathbf{u}\mathbf{u}^\dagger + \mathbf{C})^{-1}(\mathbf{z} - \alpha \mathbf{v})(\mathbf{z} - \alpha \mathbf{v})^\dagger + \mathbf{C}^{-1}\mathbf{S}]}]}{\pi^{N(K+1)} \det^K(\mathbf{C}) \det(\nu \mathbf{u}\mathbf{u}^\dagger + \mathbf{C})} \quad (7)$$

and

$$f_0(\mathbf{z}, \mathbf{S} | \mathbf{C}) = \frac{1}{\pi^{N(K+1)}} \frac{1}{\det^{K+1}(\mathbf{C})} e^{-\text{tr}\{\mathbf{C}^{-1}[\mathbf{z}\mathbf{z}^\dagger + \mathbf{S}]\}}$$

are the probability density functions (PDFs) of $\mathbf{z}, \mathbf{r}_1, \dots, \mathbf{r}_K$ under H_1 and H_0 , respectively, and \mathbf{S}/K the sample covariance matrix computed on the secondary data, i.e.,

$$\mathbf{S} = \sum_{k=1}^K \mathbf{r}_k \mathbf{r}_k^\dagger.$$

As to η , it is the detection threshold to be set according to the desired probability of false alarm (P_{fa}). Maximization over \mathbf{C} of the likelihood under H_0 can be performed as in [3]; in fact, the maximizer of the likelihood is given by

$$\widehat{\mathbf{C}}_0 = \frac{1}{K+1} [\mathbf{z}\mathbf{z}^\dagger + \mathbf{S}].$$

It follows that

$$f_0(\mathbf{z}, \mathbf{S} | \widehat{\mathbf{C}}_0) = \left(\frac{K+1}{e\pi} \right)^{N(K+1)} [\det(\mathbf{z}\mathbf{z}^\dagger + \mathbf{S})]^{-(K+1)}. \quad (8)$$

Computation of the numerator of the GLRT and, in particular, maximization of $f_1(\mathbf{z}, \mathbf{S} | \mathbf{C}, \nu, \alpha)$ with respect to \mathbf{C} is less standard. However, it can be conducted exploiting the following result (a special case of the one in [23]).

Proposition 1: Assume that \mathbf{u} is a unit-norm vector (and that $K \geq N$). Then, for the likelihood under the H_1 hypothesis, given by equation (7), the following equality holds true

$$l_{\max} = \max_{\mathbf{C} > 0, \nu \geq 0, \alpha \in \mathbb{C}} f_1(\mathbf{z}, \mathbf{S} | \mathbf{C}, \nu, \alpha)$$

²This amounts to assuming that $\mathbf{z} = (\alpha + \epsilon)\mathbf{v} + \mathbf{n}$ where ϵ is a zero-mean complex normal random variable with unknown power ν , independent of \mathbf{n} .

$$= \max_{b \geq 0} \max_{\alpha \in \mathbb{C}} \frac{\left(\frac{K+1}{\pi e} \right)^{N(K+1)} (1+b)^{-1}}{\left[\det(\mathbf{S}) \left(1 + (\mathbf{z} - \alpha \mathbf{v})^\dagger \mathbf{S}^{-1} (\mathbf{z} - \alpha \mathbf{v}) \right) \right]^{K+1}} \times \left[\frac{\mathbf{u}^\dagger \left(\mathbf{S} + (1+b)^{-1} (\mathbf{z} - \alpha \mathbf{v})(\mathbf{z} - \alpha \mathbf{v})^\dagger \right)^{-1} \mathbf{u}}{\mathbf{u}^\dagger \left(\mathbf{S} + (\mathbf{z} - \alpha \mathbf{v})(\mathbf{z} - \alpha \mathbf{v})^\dagger \right)^{-1} \mathbf{u}} \right]^{K+1}$$

where $b = \nu \mathbf{u}^\dagger \mathbf{C}^{-1} \mathbf{u}$.

Proof: The result is a special case of the one in [23] letting therein, in equation (39), $\mathbf{R} = \mathbf{C}$, $T_p = 1$, $T_s = K$ (hence, $T_t = K+1$), $M = N$, $\mathbf{X} = \mathbf{z} - \alpha \mathbf{v}$, $\mathbf{S}_y = \mathbf{S}$, $\mathbf{v} = \mathbf{u}$, $P = \nu$. ■

In the following, we will denote by $l(b, \alpha)$ the partially-compressed likelihood under H_1 , i.e.,

$$l(b, \alpha) = \frac{\left(\frac{K+1}{\pi e} \right)^{N(K+1)} (1+b)^{-1}}{\det^{K+1}(\mathbf{S}) \left(1 + (\mathbf{z} - \alpha \mathbf{v})^\dagger \mathbf{S}^{-1} (\mathbf{z} - \alpha \mathbf{v}) \right)^{K+1}} \times \left[\frac{\mathbf{u}^\dagger \left(\mathbf{S} + (1+b)^{-1} (\mathbf{z} - \alpha \mathbf{v})(\mathbf{z} - \alpha \mathbf{v})^\dagger \right)^{-1} \mathbf{u}}{\mathbf{u}^\dagger \left(\mathbf{S} + (\mathbf{z} - \alpha \mathbf{v})(\mathbf{z} - \alpha \mathbf{v})^\dagger \right)^{-1} \mathbf{u}} \right]^{K+1}.$$

As shown in Appendix A, it can also be re-written as

$$l(b, \alpha) = \frac{\left(\frac{K+1}{\pi e} \right)^{N(K+1)} (1+b)^{-1}}{\det^{K+1}(\mathbf{S}) \left(1 + b + \|\tilde{\mathbf{z}} - \alpha \tilde{\mathbf{v}}\|^2 \right)^{K+1}} \times \left[\frac{(1+b) + \|\mathbf{P}_{\tilde{\mathbf{u}}}^\perp (\tilde{\mathbf{z}} - \alpha \tilde{\mathbf{v}})\|^2}{1 + \|\mathbf{P}_{\tilde{\mathbf{u}}}^\perp (\tilde{\mathbf{z}} - \alpha \tilde{\mathbf{v}})\|^2} \right]^{K+1} \quad (9)$$

where $\tilde{\mathbf{z}} = \mathbf{S}^{-1/2} \mathbf{z}$, $\tilde{\mathbf{v}} = \mathbf{S}^{-1/2} \mathbf{v}$, and $\tilde{\mathbf{u}} = \mathbf{S}^{-1/2} \mathbf{u}$ are the “whitened” versions of \mathbf{z} , \mathbf{v} , and \mathbf{u} , respectively, and we recall that $\mathbf{P}_{\tilde{\mathbf{u}}}^\perp$ is the (orthogonal) projection matrix onto the orthogonal complement of the subspace spanned by $\tilde{\mathbf{u}}$.

For $\mathbf{u} = \mathbf{v}$, $l(b, \alpha)$ can be easily maximized and the GLRT is Kelly's detector (ref. Appendix A). If, instead, $\mathbf{u} \neq \mathbf{v}$, maximization of the above partially-compressed likelihood with respect to $\alpha \in \mathbb{C}$ can be restricted to a proper “segment” of the complex plane. In fact, the following result holds true.

Proposition 2: Let $\mathbf{P}_{\tilde{\mathbf{u}}}^\perp \tilde{\mathbf{v}} \neq \mathbf{0}$. The maximum of the function $l(b, \alpha)$ with respect to $\alpha \in \mathbb{C}$, given $b \geq 0$, is attained over the segment whose endpoints are α_1 and α_2 , defined as

$$\alpha_1 = \arg \min_{\alpha} (\tilde{\mathbf{z}} - \alpha \tilde{\mathbf{v}})^\dagger (\tilde{\mathbf{z}} - \alpha \tilde{\mathbf{v}}) = (\tilde{\mathbf{v}}^\dagger \tilde{\mathbf{v}})^{-1} \tilde{\mathbf{v}}^\dagger \tilde{\mathbf{z}}$$

$$\alpha_2 = \arg \min_{\alpha} \|\mathbf{P}_{\tilde{\mathbf{u}}}^\perp (\tilde{\mathbf{z}} - \alpha \tilde{\mathbf{v}})\|^2 = (\tilde{\mathbf{v}}^\dagger \mathbf{P}_{\tilde{\mathbf{u}}}^\perp \tilde{\mathbf{v}})^{-1} \tilde{\mathbf{v}}^\dagger \mathbf{P}_{\tilde{\mathbf{u}}}^\perp \tilde{\mathbf{z}}.$$

Proof: See Appendix A. ■

From the proposition above, α can be re-written as

$$\alpha(t) = t\alpha_1 + (1-t)\alpha_2, \quad t \in [0, 1].$$

Accordingly, we have

$$|\alpha(t) - \alpha_1|^2 = |t\alpha_1 + (1-t)\alpha_2 - \alpha_1|^2 = (1-t)^2 |\alpha_2 - \alpha_1|^2,$$

$$|\alpha(t) - \alpha_2|^2 = |t\alpha_1 + (1-t)\alpha_2 - \alpha_2|^2 = t^2 |\alpha_1 - \alpha_2|^2;$$

then, using equations (A.16), (A.18), and (A.19), together with the above two equations, yields

$$\begin{aligned}
l(b, \alpha(t)) &= \left(\frac{K+1}{\pi e} \right)^{N(K+1)} \frac{1}{\det^{K+1}(\mathbf{S})} \\
&\quad \times l_1 \left(b, \|\tilde{\mathbf{z}} - \alpha(t)\tilde{\mathbf{v}}\|^2 \right) l_2 \left(b, \|\mathbf{P}_{\tilde{\mathbf{u}}}^\perp (\tilde{\mathbf{z}} - \alpha(t)\tilde{\mathbf{v}})\|^2 \right) \\
&= \left(\frac{K+1}{\pi e} \right)^{N(K+1)} \frac{1}{\det^{K+1}(\mathbf{S})} \\
&\quad \times l_1 \left(b, \tilde{\mathbf{z}}^\dagger \mathbf{P}_{\tilde{\mathbf{v}}}^\perp \tilde{\mathbf{z}} + (1-t)^2 |\alpha_2 - \alpha_1|^2 \tilde{\mathbf{v}}^\dagger \tilde{\mathbf{v}} \right) \\
&\quad \times l_2 \left(b, \tilde{\mathbf{z}}^\dagger \mathbf{P}_{\tilde{\mathbf{u}}}^\perp \mathbf{P}_{\tilde{\mathbf{v}}}^\perp \mathbf{P}_{\tilde{\mathbf{u}}}^\perp \tilde{\mathbf{z}} + t^2 |\alpha_1 - \alpha_2|^2 \tilde{\mathbf{v}}^\dagger \mathbf{P}_{\tilde{\mathbf{u}}}^\perp \tilde{\mathbf{v}} \right)
\end{aligned}$$

with $l_1(\cdot, \cdot)$ and $l_2(\cdot, \cdot)$ given in equation (A.17). Summarizing, the GLRT can be written as

$$\frac{\max_{b \geq 0} \max_{t \in [0,1]} l(b, \alpha(t))}{\left(\frac{K+1}{\pi e} \right)^{N(K+1)} \frac{1}{\det^{K+1}(\mathbf{S})} (1 + \mathbf{z}^\dagger \mathbf{S}^{-1} \mathbf{z})^{-(K+1)}} \underset{H_0}{\overset{H_1}{>}} \eta$$

and also as

$$\begin{aligned}
&\max_{b \geq 0} \max_{t \in [0,1]} \frac{l_1 \left(b, \tilde{\mathbf{z}}^\dagger \mathbf{P}_{\tilde{\mathbf{v}}}^\perp \tilde{\mathbf{z}} + (1-t)^2 R^2 \tilde{\mathbf{v}}^\dagger \tilde{\mathbf{v}} \right)}{(1 + \mathbf{z}^\dagger \mathbf{S}^{-1} \mathbf{z})^{-(K+1)}} \\
&\quad \times l_2 \left(b, \tilde{\mathbf{z}}^\dagger \mathbf{P}_{\tilde{\mathbf{u}}}^\perp \mathbf{P}_{\tilde{\mathbf{v}}}^\perp \mathbf{P}_{\tilde{\mathbf{u}}}^\perp \tilde{\mathbf{z}} + t^2 R^2 \tilde{\mathbf{v}}^\dagger \mathbf{P}_{\tilde{\mathbf{u}}}^\perp \tilde{\mathbf{v}} \right) \underset{H_0}{\overset{H_1}{>}} \eta \quad (10)
\end{aligned}$$

where $R^2 = |\alpha_1 - \alpha_2|^2$. Equation (10) is a computationally more convenient alternative for the GLRT in the case $\Sigma = \mathbf{u}\mathbf{u}^\dagger$, with \mathbf{u} any chosen vector. This rewriting is in fact less demanding than using $l(b, \alpha)$ for the numerator (partially-compressed likelihood under H_1): in particular, the maximization over $\alpha \in \mathbb{C}$ of $l(b, \alpha)$ (e.g., using equation (9)) would require a complex-valued (two-dimensional) unbounded optimization instead of the simple scalar search of t in the finite interval $[0, 1]$ appearing in (10). Moreover, it is reasonable to constraint b to belong to a finite interval, say $[0, b_{\max}]$. This further reduces the ultimate complexity and makes it possible to implement the detector using a numerical algorithm with box constraints or, alternatively, a grid search.

B. Case 2: Derivation of the GLRT for $\Sigma = \mathbf{C}$

In this case Σ is unknown, but equal to the covariance matrix of the noise \mathbf{C} . Clearly, since the latter is unrelated to the sources of error producing the steering vector mismatch that we hope to capture through the random term $\boldsymbol{\theta}$, a direct physical meaning for $\Sigma = \mathbf{C}$ is missing; however, such a choice is mathematically convenient and leads to a detector with sound properties, as shown later. Also, if \mathbf{C} were known, the GLRT would process the whitened received signal and the choice $\Sigma = \mathbf{C}$ would be tantamount to modeling the random component to be added to the (whitened) steering vector as a white term. This is reasonable when no a-priori knowledge on the nature of the mismatch is available, hence $\Sigma = \mathbf{C}$ is actually a conservative (less informative) choice.³

³Please also recall the general rationale of test (4) and the discussion at the beginning of Section II.

The corresponding GLRT is

$$\Lambda(\mathbf{z}, \mathbf{S}) = \frac{\max_{\mathbf{C} > 0} \max_{\nu \geq 0} \max_{\alpha \in \mathbb{C}} f_1(\mathbf{z}, \mathbf{S} | \mathbf{C}, \nu, \alpha)}{\max_{\mathbf{C} > 0} f_0(\mathbf{z}, \mathbf{S} | \mathbf{C})} \underset{H_0}{\overset{H_1}{>}} \eta \quad (11)$$

where

$$f_1(\mathbf{z}, \mathbf{S} | \mathbf{C}, \nu, \alpha) = \frac{e^{-\text{tr} \{ \mathbf{C}^{-1} [\frac{1}{1+\nu} (\mathbf{z} - \alpha \mathbf{v})(\mathbf{z} - \alpha \mathbf{v})^\dagger + \mathbf{S}] \}}}{\pi^{N(K+1)} (1 + \nu)^N \det^{K+1}(\mathbf{C})}$$

is the PDF of $\mathbf{z}, \mathbf{r}_1, \dots, \mathbf{r}_K$ under H_1 while the denominator of (11) is given by (8). Again η is the detection threshold for the desired P_{fa} . We also recall that \mathbf{S} is K times the sample covariance matrix computed on the secondary data.

Maximization over \mathbf{C} of the likelihood under H_1 can be performed as in [3]; in fact, we have that

$$\hat{\mathbf{C}}_1(\nu, \alpha) = \frac{1}{K+1} \left[\frac{1}{1+\nu} (\mathbf{z} - \alpha \mathbf{v})(\mathbf{z} - \alpha \mathbf{v})^\dagger + \mathbf{S} \right].$$

Thus, the partially-compressed likelihood under H_1 becomes

$$\begin{aligned}
f_1(\mathbf{z}, \mathbf{S} | \hat{\mathbf{C}}_1(\nu, \alpha), \nu, \alpha) &= \left(\frac{K+1}{e\pi} \right)^{N(K+1)} \\
&\quad \times \frac{1}{(1+\nu)^N} \left[\det \left(\frac{1}{1+\nu} (\mathbf{z} - \alpha \mathbf{v})(\mathbf{z} - \alpha \mathbf{v})^\dagger + \mathbf{S} \right) \right]^{-(K+1)}.
\end{aligned}$$

Plugging the above expressions into equation (11) yields

$$\Lambda^{\frac{1}{K+1}}(\mathbf{z}, \mathbf{S}) = \frac{1 + \|\tilde{\mathbf{z}}\|^2}{\min_{\nu \geq 0, \alpha \in \mathbb{C}} (1 + \nu)^{\frac{N}{K+1}} \left[1 + \frac{1}{1+\nu} \|\tilde{\mathbf{z}} - \alpha \tilde{\mathbf{v}}\|^2 \right]}.$$

Moreover, minimization over α leads to [25]

$$\Lambda^{\frac{1}{K+1}}(\mathbf{z}, \mathbf{S}) = \frac{1 + \|\tilde{\mathbf{z}}\|^2}{\min_{\nu \geq 0} (1 + \nu)^{\frac{N}{K+1}} \left[1 + \frac{1}{1+\nu} \|\mathbf{P}_{\tilde{\mathbf{v}}}^\perp \tilde{\mathbf{z}}\|^2 \right]}.$$

Minimization of denominator with respect to ν can be easily accomplished using the following proposition.

Proposition 3: The function

$$f(\nu) = (1 + \nu)^{\frac{N}{K+1}} \left(1 + \frac{a}{1+\nu} \right), \quad a > 0, K \geq N$$

admits a unique minimum over $[0, +\infty)$ at

$$\hat{\nu} = \begin{cases} \left(\frac{K+1}{N} - 1 \right) a - 1, & \left(\frac{K+1}{N} - 1 \right) a - 1 > 0 \\ 0, & \text{otherwise} \end{cases}$$

given by

$$f_{\min} = \begin{cases} \left(\frac{K+1-N}{N} a \right)^{\frac{N}{K+1}} \frac{K+1}{K+1-N}, & \frac{K+1-N}{N} a > 1 \\ 1 + a, & \text{otherwise} \end{cases}.$$

Proof: See Appendix B. ■

Thus, it follows that the GLRT can be written as

$$\Lambda_0(\mathbf{z}, \mathbf{S}) = \Lambda^{\frac{1}{K+1}}(\mathbf{z}, \mathbf{S}) \underset{H_0}{\overset{H_1}{>}} \eta \quad (12)$$

where

$$\Lambda_0(\mathbf{z}, \mathbf{S}) = \begin{cases} \frac{\left(1 + \|\tilde{\mathbf{z}}\|^2\right) \left(1 - \frac{1}{\zeta}\right)}{\frac{1}{\zeta}}, & \|\mathbf{P}_{\tilde{\mathbf{v}}}^\perp \tilde{\mathbf{z}}\|^2 > \frac{1}{\zeta - 1} \\ \left[(\zeta - 1) \|\mathbf{P}_{\tilde{\mathbf{v}}}^\perp \tilde{\mathbf{z}}\|^2 \right] \bar{\zeta} & \\ \frac{1 + \|\tilde{\mathbf{z}}\|^2}{1 + \|\mathbf{P}_{\tilde{\mathbf{v}}}^\perp \tilde{\mathbf{z}}\|^2}, & \text{otherwise} \end{cases}$$

$\zeta = \frac{K+1}{N}$, and η denotes a modification of the original threshold. The P_{fa} of the test and the characterization of the decision statistic under H_1 can be obtained in closed form, and are reported in Appendix B. Remarkably, in the appendix it is shown that the detector has the desirable CFAR property.

Notice that, conditionally to

$$\|\mathbf{P}_{\tilde{\mathbf{v}}}^\perp \tilde{\mathbf{z}}\|^2 < \frac{1}{\zeta - 1} \quad (13)$$

$\Lambda_0(\mathbf{z}, \mathbf{S})$ is equivalent to Kelly's statistic; it turns out that the detector robustness comes from $\Lambda_0(\mathbf{z}, \mathbf{S})$ under the condition complementary to (13). Thus, it seems possible to promote robustness by decreasing the probability to select "Kelly's statistic". In particular, we propose to replace ζ in (13) with

$$\zeta_\epsilon = \frac{K+1}{N} (1 + \epsilon), \quad \epsilon \geq 0. \quad (14)$$

We made this ad-hoc substitution also on the decision statistic, obtaining the following parametric detector that thus generalizes (12) through (14):

$$\Lambda_\epsilon(\mathbf{z}, \mathbf{S}) \underset{H_0}{\overset{H_1}{>}} \eta \quad (15)$$

where

$$\Lambda_\epsilon(\mathbf{z}, \mathbf{S}) = \begin{cases} \frac{\left(1 + \|\tilde{\mathbf{z}}\|^2\right) \left(1 - \frac{1}{\zeta_\epsilon}\right)}{\frac{1}{\zeta_\epsilon}}, & \|\mathbf{P}_{\tilde{\mathbf{v}}}^\perp \tilde{\mathbf{z}}\|^2 > \frac{1}{\zeta_\epsilon - 1} \\ \left[(\zeta_\epsilon - 1) \|\mathbf{P}_{\tilde{\mathbf{v}}}^\perp \tilde{\mathbf{z}}\|^2 \right] \bar{\zeta}_\epsilon & \\ \frac{1 + \|\tilde{\mathbf{z}}\|^2}{1 + \|\mathbf{P}_{\tilde{\mathbf{v}}}^\perp \tilde{\mathbf{z}}\|^2}, & \text{otherwise.} \end{cases}$$

Such parametric detector encompasses detector (12) for $\epsilon = 0$ and eventually $\zeta_\epsilon = \zeta$. Moreover, we will show that detector (15) can outperform detector (12) in terms of robustness, without incurring additional loss under matched conditions. Finally, a closed form for its P_{fa} is given in equation (B.24) of Appendix B, which allows one to set the threshold to guarantee the desired P_{fa} for any choice of ϵ ; for convenience, the curves for some relevant values of ϵ are drawn in Fig. 1, also revealing that the P_{fa} does not significantly change with ϵ . In Appendix B it is furthermore proven that the proposed detector (15) (hence also (12)) possesses the CFAR property, i.e., its P_{fa} does not depend on any unknown parameter (including the unknown noise covariance matrix \mathbf{C}); additionally, it is proven that its performance in terms of P_d depends only on the SNR (equation (B.25)) and the cosine squared $\cos^2 \theta$ (equation (B.26)) between the nominal steering vector and the actual one, which are the same performance parameters of Kelly's, AMF, Kalson's, and KWA detectors. This remarkable fact corroborates the soundness and

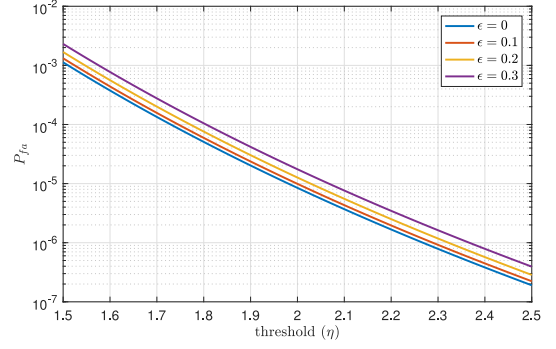


Fig. 1. Curves of P_{fa} vs detection threshold, for different values of ϵ .

convenience of the choice $\Sigma = \mathbf{C}$. It also means that P_d does not depend directly on noise-related parameters, namely the clutter power and correlation, but only through SNR and $\cos^2 \theta$; as a consequence, the figures we will provide in Section III (P_d vs SNR for different $\cos^2 \theta$) are quite representative of the general performance, despite they are obtained for a specific choice of \mathbf{C} .

C. Discussion

It is important to stress that the derivation of the GLRT for $\Sigma = \mathbf{C}$ and, hence, the result is different from the detector proposed in [6]. More precisely, considering the derivation of the ACE as the GLRT to detect a possible coherent signal in presence of partially-homogeneous noise, given in [6], we highlight that therein the parameter ν represents the possible mismatch between the power of the noise in the data under test and that of secondary data. Herein, instead, ν enters the characterization of a possible random mismatch between the actual and the nominal useful signal. For this reason, we have $1 + \nu$ in place of ν under H_1 ($\nu\mathbf{C}$ stands for the covariance matrix of the random term) and, in addition, ν is not present under the H_0 hypothesis. This difference in the formulation of the hypothesis testing problem makes our detector more robust than Kelly's detector [3] in presence of mismatched signals while it is well-known that the ACE is more selective than the latter (under the same operating conditions).

Table I reports a summary of the proposed detectors for test (5), also in comparison with the classical approach (test (2)).⁴

III. PERFORMANCE ANALYSIS

We assume a time steering vector, i.e., $\mathbf{v} = [1 \ e^{i2\pi f_d} \dots \ e^{i2\pi(N-1)f_d}]^T$, with $N = 16$ and normalized Doppler frequency $f_d = 0.08$, a small value such that the target competes with low pass clutter. The target amplitude α is generated deterministically according to the SNR defined in equation (B.25). To assess the robustness of the proposed detectors, we simulate a target with a mismatched steering vector, say \mathbf{p} , having normalized Doppler frequency $f_d + \delta_f$ with $\delta_f \in \{0.2/N, 0.4/N\}$.

⁴For completeness, we mention that [24] provides the general derivation (for any Σ) and a closed-form for $\Sigma = \mathbf{C}$ following the two-step GLRT approach, namely deriving the GLRT for known \mathbf{C} and then using as replacement an estimate $\hat{\mathbf{C}}$ (from secondary data); such detectors are however less powerful than one-step GLRTs. In Appendix C we show that for $\Sigma = \mathbf{v}\mathbf{v}^\dagger$ the two-step GLRT is equivalent to the AMF, whereas the proposed one-step GLRT for the same choice of Σ is equivalent to Kelly's detector (ref. Section II-A).

TABLE I
SUMMARY OF PROPOSED DETECTORS FOR TEST (5) AND COMPARISON WITH THE CLASSICAL APPROACH (TEST (2))

	no random term (classical test (2))	general Σ	$\Sigma = uu^\dagger$ (general u)	$\Sigma = vv^\dagger$	$\Sigma = C$
one-step GLRT	Kelly's detector	–	eq. (10)	Kelly's detector	eq. (12); parametric generalization eq. (15)
two-step GLRT	AMF	eq. (9) in [24]	eq. (9) in [24]	AMF	eq. (11) in [24]

The values of δ_f will affect the values of the cosine squared of the angle between the nominal steering vector and the mismatched one, denoted by $\cos^2 \theta$ and given in equation (B.26), which is a standard way to quantify the mismatch in radar detection. Under matched conditions, of course, $p = v$ and $\cos^2 \theta = 1$.

We model the noise component of z and the r_k 's as (independent) random vectors ruled by a zero-mean, complex Gaussian distribution. As to the covariance matrix, we adopt as C the sum of a Gaussian-shaped clutter covariance matrix and white (thermal) noise 10 dB weaker, i.e., $C = R_c + \sigma_n^2 I_N$ with the (m_1, m_2) th element of the matrix R_c given by $[R_c]_{m_1, m_2} \propto \exp\{-2\pi^2 \sigma_f^2 (m_1 - m_2)^2\}$ and $\sigma_f \approx 0.073$ (corresponding to a one-lag correlation coefficient of the clutter component equal to 0.9).

In the following we assess the performance of the proposed (one-step) GLRTs, considering both $\Sigma = v_m v_m^\dagger$ and $\Sigma = C$, and the parametric detector (15). The former detector assumes as v_m a slightly mismatched version of v , in particular of $0.03/N$, and for the optimization with respect to b we adopt a logarithmic search in the span $[0, b_{\max} = 10^3]$; as regards the parametric detector (15), we consider $\epsilon = 0.1$ and $\epsilon = 0.2$. It will be apparent from the simulations below that such choices guarantee negligible loss with respect to Kelly's detector under matched conditions.

A comparison is performed against the natural competitors for the problem at hand, that is the Kalson's [10] and KWA [11] tunable receivers. Notice that for both such competitors, the level of robustness increases as the value of their tunable parameter decreases. For a fair comparison, only values that ensure practically the same performance of Kelly's detector under matched conditions are considered, in particular $\beta = 0.5$ and $\beta = 0.8$ for Kalson's detector and $\gamma = 0.45$ and $\gamma = 0.4$ for the KWA. For reference, the AMF [5] is also reported in all figures, because it is a well-known robust detector; however, it is worth remarking that it is not always a competitor, since it generally experiences a performance loss under matched conditions with respect to Kelly's detector.

A first set of simulations (Figs. 2–4) refers to $P_{fa} = 10^{-4}$. We assess performance by Monte Carlo simulation with $100/P_{fa}$ independent trials to set the thresholds and 10^3 independent trials to compute the P_d 's (the probabilities to decide for H_1 when a useful signal is present). Results under matched conditions are reported in Fig. 2 for different values of the number of secondary data, namely $K = 24, 32, 40$ respectively (i.e., besides the typical $K = 2N$, also $1.5N$ and $2.5N$ are considered). From such figures, it is apparent that the proposed detectors and the tunable competitors (Kalson's and KWA) have essentially the same P_d of Kelly's detector, while as known the AMF exhibits a performance loss, which becomes negligible only when the number of secondary data is large enough. Notice that the KWA for $\gamma = 0.4$ and the detector (15) for $\epsilon = 0.2$ start to experience some loss, especially for moderate SNR, hence smaller values

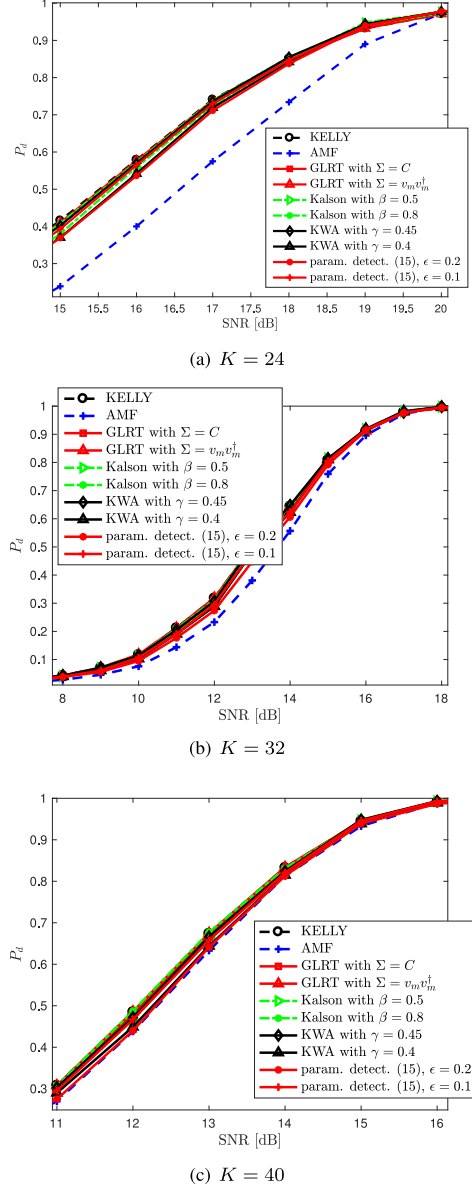


Fig. 2. P_d vs SNR under matched conditions, for $P_{fa} = 10^{-4}$.

of their respective parameters are not considered for a fair comparison.

Fig. 3 reports the results under mismatch, in particular considering a cosine squared of the angle between the nominal steering vector and the mismatched one (given by equation (B.26)) equal to $\cos^2 \theta \approx 0.46$ (obtained for $\delta_f = 0.4/N = 0.025$). It emerges that the proposed approach yields a family of robust receivers, whose performance in terms of robustness to mismatches depends on the design matrix Σ and number of secondary data K . The behavior of the GLRT for $\Sigma = C$ is very interesting,

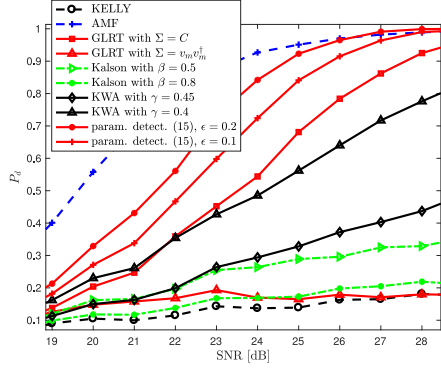
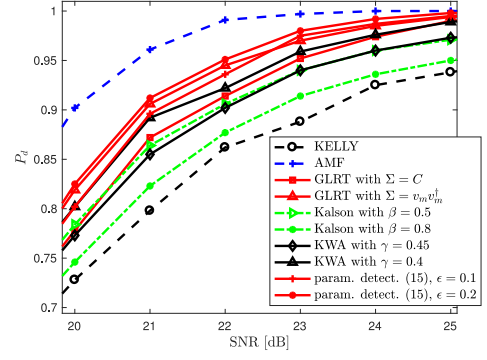
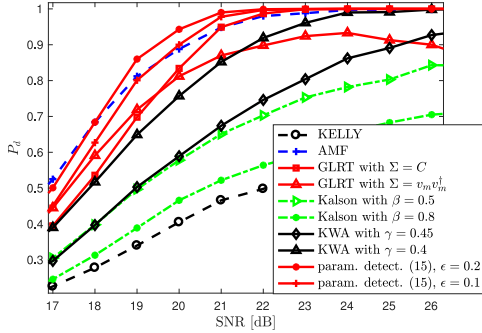
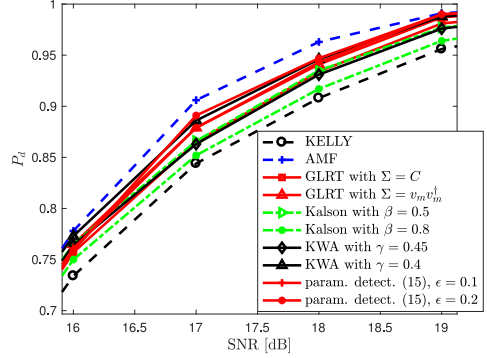
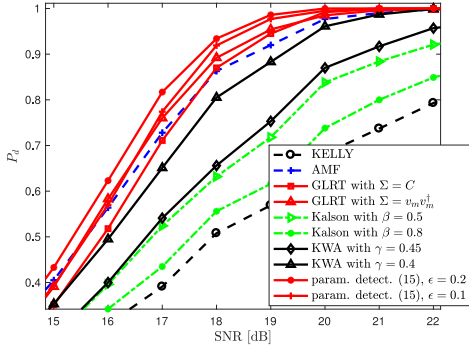
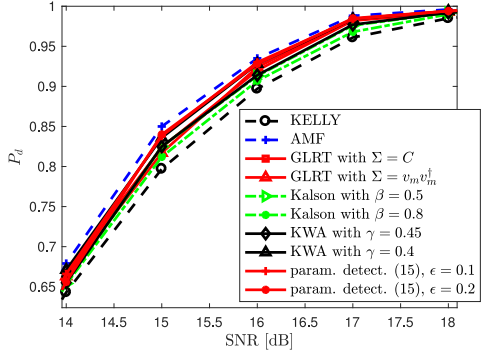
(a) $K = 24$ (a) $K = 24$ (b) $K = 32$ (b) $K = 32$ (c) $K = 40$ (c) $K = 40$

Fig. 3. P_d vs SNR in case of mismatched steering vector, for $\cos^2 \theta \approx 0.46$ and $P_{fa} = 10^{-4}$.

Fig. 4. P_d vs SNR in case of mismatched steering vector, for $\cos^2 \theta \approx 0.83$ and $P_{fa} = 10^{-4}$.

because it is (equivalent to Kelly's detector under matched conditions and) more robust than Kalson's and KWA receivers; the parametric detector (15) with both settings of ϵ is more robust than the GLRT for $\Sigma = C$ and can be even more robust than AMF, in particular for $K = 32$, without the loss experienced by the latter under matched conditions. This "win-win" behavior is thus remarkably unique and not achievable with state-of-the-art receivers. Notice that the AMF can be considered a competitor only for $K = 40$ (where its performance loss under matched conditions compared to Kelly's detector becomes very small), but Fig. 3(c) shows that the proposed detectors, in particular the GLRT for $\Sigma = C$ and the parametric detector (15) with both settings of ϵ , are more robust than AMF; notice that this advantage comes at no increase in computational complexity.

The GLRT with $\Sigma = v_m v_m^\dagger$ needs higher values of K to achieve almost the same robustness of the other proposed receivers (Fig. 3(c)); otherwise, it progressively rejects the H_1 hypothesis: for $K = 32$ (Fig. 3(b)) only for larger SNR (not shown in the figure), for $K = 24$ (Fig. 3(a)) behaving as a selective receiver over the whole range of SNRs. As to Kalson's detector, for $\beta = 0.8$ it is close to Kelly's detector (in particular for $K = 24$).

For a reduced value of the mismatch, the differences between the proposed detectors and the competitors reduce. Fig. 4 shows the mismatched case with $\cos^2 \theta \approx 0.83$ (obtained for $\delta_f = 0.2/N = 0.0125$). We observe that the parametric detector (15) still emerges as the most robust among the detectors that have negligible loss under matched conditions (compared to Kelly's

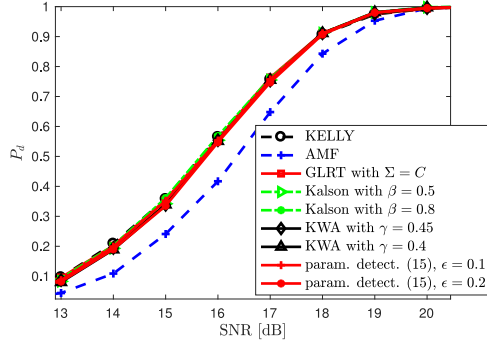


Fig. 5. P_d vs SNR in case of matched steering vector, for $K = 32$, and $P_{fa} = 10^{-6}$.

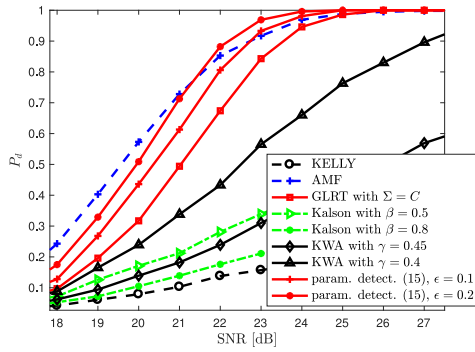


Fig. 6. P_d vs SNR in case of mismatched steering vector, for $K = 32$, $\cos^2 \theta \approx 0.46$, and $P_{fa} = 10^{-6}$.

detector) hence excluding AMF for $K = 24, 32$; for $K = 40$, conversely, the detector (15) and AMF are almost equivalent.

A second set of simulations (Figs. 5–6) refers to $P_{fa} = 10^{-6}$ and focuses on the behavior of the proposed GLRT for $\Sigma = C$ and the parametric detector (15) in comparison to Kalson’s and KWA detectors; for reference, also the performance of Kelly’s detector and AMF are shown. Notice that, for such a small P_{fa} , Monte Carlo simulations are prohibitively long, hence we can compare only detectors for which a closed-form expression is available for the relationship between the threshold and the P_{fa} ; for this reason the proposed GLRT with $\Sigma = v_m v_m^\dagger$ cannot be included; besides, the detector with $\Sigma = C$ and the parametric detector (15) are simpler and show a more interesting behavior, hence are more appealing for applications. Again we resort to Monte Carlo simulation and to 10^3 independent trials to estimate the P_d s. The values of the tunable parameters for the parametric detector and the competitors are chosen as before, because this guarantees no appreciable loss under matched conditions as shown in Fig. 5. In Fig. 6 we report the results under mismatched conditions for $\cos^2 \theta \approx 0.46$ and $K = 32$. Comparing the result with the corresponding Fig. 3(b), the better performance of the proposed receivers are even more evident. We see that they are more robust than Kalson’s and KWA detectors; in particular, the parametric detector with $\epsilon = 0.2$ is also more robust than the AMF for large SNR values while Kalson’s detector with $\beta = 0.8$ approaches the selective behavior of Kelly’s detector.

IV. CONCLUSION

We have proposed a novel family of robust radar receivers to detect the possible presence of a coherent return from a given cell under test mismatched with respect to the nominal steering vector. To this end, we have introduced a random component in addition to the deterministic useful signal; the random component has a given structure Σ , but its power ν is estimated from the data. This likely produces an estimate of ν close to zero under matched conditions, thus achieving no loss compared to Kelly’s detector (which is the benchmark for the considered problem). We have solved the hypothesis testing problem resorting to the GLRT approach and assuming for Σ either a known rank-one matrix or the unknown covariance matrix of the noise. We have also introduced a parametric detector that naturally modifies the statistic of the latter GLRT and shares with it the CFAR property. The performance analysis has shown that proposed detectors are a viable means to deal with mismatched signals; in fact, compared to competitors that have negligible loss under matched conditions, the proposed approach guarantees an increased robustness.

Outgrowths of this work are the investigation of further possible structures for the design matrix Σ , and possibly the derivation of the one-step GLRT for the general case (which in fact is missing in Table I). A different avenue for possible generalizations is robust detection of range-spread targets; to date, the GLRT for the proposed random perturbation approach has been derived only in the case $\Sigma = C$, which though has the same remarkable properties of the point-like detector derived here [30]. Finally, it would be interesting to ascertain whether receivers with the same detection power of Kelly’s detector (under matched conditions) but controllable robustness or selectivity under mismatched conditions can be obtained through design approaches different from GLRT, namely inspired to machine learning tools.

APPENDIX A DERIVATION OF EQUATION (9)

First observe that, by the matrix inversion lemma, we have

$$\begin{aligned} & \mathbf{u}^\dagger \left(\mathbf{S} + (1+b)^{-1} (\mathbf{z} - \alpha \mathbf{v})(\mathbf{z} - \alpha \mathbf{v})^\dagger \right)^{-1} \mathbf{u} \\ &= \mathbf{u}^\dagger \mathbf{S}^{-1} \mathbf{u} - \frac{(1+b)^{-1} |\mathbf{u}^\dagger \mathbf{S}^{-1} (\mathbf{z} - \alpha \mathbf{v})|^2}{1 + (1+b)^{-1} (\mathbf{z} - \alpha \mathbf{v})^\dagger \mathbf{S}^{-1} (\mathbf{z} - \alpha \mathbf{v})}. \end{aligned}$$

Thus, $l(b, \alpha)$ can be re-written as

$$\begin{aligned} l(b, \alpha) &= \frac{\left(\frac{K+1}{\pi e}\right)^{N(K+1)} (1+b)^{-1}}{\det^{K+1}(\mathbf{S}) \left(1 + (\tilde{\mathbf{z}} - \alpha \tilde{\mathbf{v}})^\dagger (\tilde{\mathbf{z}} - \alpha \tilde{\mathbf{v}})\right)^{K+1}} \\ &\times \left[\frac{\tilde{\mathbf{u}}^\dagger \tilde{\mathbf{u}} - (1+b)^{-1} \frac{|\tilde{\mathbf{u}}^\dagger (\tilde{\mathbf{z}} - \alpha \tilde{\mathbf{v}})|^2}{1 + (1+b)^{-1} (\tilde{\mathbf{z}} - \alpha \tilde{\mathbf{v}})^\dagger (\tilde{\mathbf{z}} - \alpha \tilde{\mathbf{v}})}}{\tilde{\mathbf{u}}^\dagger \tilde{\mathbf{u}} - \frac{|\tilde{\mathbf{u}}^\dagger (\tilde{\mathbf{z}} - \alpha \tilde{\mathbf{v}})|^2}{1 + (\tilde{\mathbf{z}} - \alpha \tilde{\mathbf{v}})^\dagger (\tilde{\mathbf{z}} - \alpha \tilde{\mathbf{v}})}} \right]^{K+1} \end{aligned}$$

where $\tilde{\mathbf{z}} = \mathbf{S}^{-1/2} \mathbf{z}$, $\tilde{\mathbf{v}} = \mathbf{S}^{-1/2} \mathbf{v}$, and $\tilde{\mathbf{u}} = \mathbf{S}^{-1/2} \mathbf{u}$ are the whitened versions of \mathbf{z} , \mathbf{v} , and \mathbf{u} , respectively.

Notice also that

$$\begin{aligned}
& \frac{\tilde{\mathbf{u}}^\dagger \tilde{\mathbf{u}} - (1+b)^{-1} \frac{|\tilde{\mathbf{u}}^\dagger(\tilde{\mathbf{z}} - \alpha \tilde{\mathbf{v}})|^2}{1+(1+b)^{-1}(\tilde{\mathbf{z}} - \alpha \tilde{\mathbf{v}})^\dagger(\tilde{\mathbf{z}} - \alpha \tilde{\mathbf{v}})}}{\tilde{\mathbf{u}}^\dagger \tilde{\mathbf{u}} - \frac{|\tilde{\mathbf{u}}^\dagger(\tilde{\mathbf{z}} - \alpha \tilde{\mathbf{v}})|^2}{1+(\tilde{\mathbf{z}} - \alpha \tilde{\mathbf{v}})^\dagger(\tilde{\mathbf{z}} - \alpha \tilde{\mathbf{v}})}} \\
&= \frac{\tilde{\mathbf{u}}^\dagger \tilde{\mathbf{u}} - \frac{|\tilde{\mathbf{u}}^\dagger(\tilde{\mathbf{z}} - \alpha \tilde{\mathbf{v}})|^2}{1+b+(\tilde{\mathbf{z}} - \alpha \tilde{\mathbf{v}})^\dagger(\tilde{\mathbf{z}} - \alpha \tilde{\mathbf{v}})}}{\tilde{\mathbf{u}}^\dagger \tilde{\mathbf{u}} - \frac{|\tilde{\mathbf{u}}^\dagger(\tilde{\mathbf{z}} - \alpha \tilde{\mathbf{v}})|^2}{1+(\tilde{\mathbf{z}} - \alpha \tilde{\mathbf{v}})^\dagger(\tilde{\mathbf{z}} - \alpha \tilde{\mathbf{v}})}} \\
&= \frac{(1+b)\tilde{\mathbf{u}}^\dagger \tilde{\mathbf{u}} + \tilde{\mathbf{u}}^\dagger \tilde{\mathbf{u}} \|\tilde{\mathbf{z}} - \alpha \tilde{\mathbf{v}}\|^2 - |\tilde{\mathbf{u}}^\dagger(\tilde{\mathbf{z}} - \alpha \tilde{\mathbf{v}})|^2}{\tilde{\mathbf{u}}^\dagger \tilde{\mathbf{u}} + \tilde{\mathbf{u}}^\dagger \tilde{\mathbf{u}} \|\tilde{\mathbf{z}} - \alpha \tilde{\mathbf{v}}\|^2 - |\tilde{\mathbf{u}}^\dagger(\tilde{\mathbf{z}} - \alpha \tilde{\mathbf{v}})|^2} \\
&\quad \times \frac{1 + (\tilde{\mathbf{z}} - \alpha \tilde{\mathbf{v}})^\dagger(\tilde{\mathbf{z}} - \alpha \tilde{\mathbf{v}})}{1 + b + (\tilde{\mathbf{z}} - \alpha \tilde{\mathbf{v}})^\dagger(\tilde{\mathbf{z}} - \alpha \tilde{\mathbf{v}})}.
\end{aligned}$$

It turns out that $l(b, \alpha)$ can be re-cast as

$$\begin{aligned}
l(b, \alpha) &= \frac{\left(\frac{K+1}{\pi e}\right)^{N(K+1)} (1+b)^{-1}}{\det^{K+1}(\mathbf{S}) \left(1 + b + (\tilde{\mathbf{z}} - \alpha \tilde{\mathbf{v}})^\dagger(\tilde{\mathbf{z}} - \alpha \tilde{\mathbf{v}})\right)^{K+1}} \\
&\quad \times \left[\frac{(1+b)\|\tilde{\mathbf{u}}\|^2 + \|\tilde{\mathbf{u}}\|^2 \|\tilde{\mathbf{z}} - \alpha \tilde{\mathbf{v}}\|^2 - |\tilde{\mathbf{u}}^\dagger(\tilde{\mathbf{z}} - \alpha \tilde{\mathbf{v}})|^2}{\|\tilde{\mathbf{u}}\|^2 + \|\tilde{\mathbf{u}}\|^2 \|\tilde{\mathbf{z}} - \alpha \tilde{\mathbf{v}}\|^2 - |\tilde{\mathbf{u}}^\dagger(\tilde{\mathbf{z}} - \alpha \tilde{\mathbf{v}})|^2} \right]^{K+1}
\end{aligned}$$

and letting $|\tilde{\mathbf{u}}^\dagger(\tilde{\mathbf{z}} - \alpha \tilde{\mathbf{v}})|^2 = \|\tilde{\mathbf{u}}\|^2 \|\mathbf{P}_{\tilde{\mathbf{u}}}(\tilde{\mathbf{z}} - \alpha \tilde{\mathbf{v}})\|^2$ it can be re-written in the form of equation (9).

THE GLRT WITH $\Sigma = \mathbf{v}\mathbf{v}^\dagger$ IS THE KELLY'S DETECTOR

If $\mathbf{u} = \mathbf{v}$ and, hence, $\mathbf{P}_{\tilde{\mathbf{u}}}^\perp \tilde{\mathbf{v}} = 0$, the partially-compressed likelihood under H_1 of equation (9) becomes

$$\begin{aligned}
l(b, \alpha) &= \frac{\left(\frac{K+1}{\pi e}\right)^{N(K+1)} (1+b)^{-1}}{\det^{K+1}(\mathbf{S}) \left(1 + b + (\tilde{\mathbf{z}} - \alpha \tilde{\mathbf{v}})^\dagger(\tilde{\mathbf{z}} - \alpha \tilde{\mathbf{v}})\right)^{K+1}} \\
&\quad \times \left[\frac{(1+b) + \|\mathbf{P}_{\tilde{\mathbf{v}}}^\perp \tilde{\mathbf{z}}\|^2}{1 + \|\mathbf{P}_{\tilde{\mathbf{v}}}^\perp \tilde{\mathbf{z}}\|^2} \right]^{K+1}
\end{aligned}$$

and

$$\max_{\alpha} l(b, \alpha) = \frac{(1+b)^{-1} \left(\frac{K+1}{\pi e}\right)^{N(K+1)}}{\det^{K+1}(\mathbf{S}) \left(1 + \|\mathbf{P}_{\tilde{\mathbf{v}}}^\perp \tilde{\mathbf{z}}\|^2\right)^{K+1}}.$$

As a consequence, we also have that

$$\max_{b \geq 0} \max_{\alpha} l(b, \alpha) = \frac{\left(\frac{K+1}{\pi e}\right)^{N(K+1)}}{\det^{K+1}(\mathbf{S}) \left(1 + \|\mathbf{P}_{\tilde{\mathbf{v}}}^\perp \tilde{\mathbf{z}}\|^2\right)^{K+1}}$$

and the GLRT, given by equation (6), can be written as

$$\frac{1 + \mathbf{z}^\dagger \mathbf{S}^{-1} \mathbf{z}}{1 + \|\mathbf{P}_{\tilde{\mathbf{v}}}^\perp \tilde{\mathbf{z}}\|^2} = \frac{1 + \mathbf{z}^\dagger \mathbf{S}^{-1} \mathbf{z}}{1 + \mathbf{z}^\dagger \mathbf{S}^{-1} \mathbf{z} - \frac{|\mathbf{v}^\dagger \mathbf{S}^{-1} \mathbf{z}|^2}{\mathbf{v}^\dagger \mathbf{S}^{-1} \mathbf{v}}} \stackrel{H_1}{<} \eta,$$

with η a proper modification of the original threshold, that is equivalent to Kelly's detector (we have also used equation (8) for the compressed likelihood under H_0).

PROOF OF PROPOSITION 2

First observe that $l(b, \alpha)$ can be written as

$$l(b, \alpha) = \frac{l_1(b, \|\tilde{\mathbf{z}} - \alpha \tilde{\mathbf{v}}\|^2) l_2(b, \|\mathbf{P}_{\tilde{\mathbf{u}}}^\perp(\tilde{\mathbf{z}} - \alpha \tilde{\mathbf{v}})\|^2)}{\left(\frac{K+1}{\pi e}\right)^{-N(K+1)} \det^{K+1}(\mathbf{S})} \quad (\text{A.16})$$

with

$$l_1(b, y_1) = \frac{(1+b)^{-1}}{(1+b+y_1)^{K+1}}, \quad l_2(b, y_2) = \left[\frac{(1+b) + y_2}{1+y_2} \right]^{K+1}. \quad (\text{A.17})$$

In particular, l_1 and l_2 are strictly decreasing function of y_1 and y_2 , respectively. Moreover, l_1 attains its maximum at

$$\alpha_1 = \arg \min_{\alpha} (\tilde{\mathbf{z}} - \alpha \tilde{\mathbf{v}})^\dagger(\tilde{\mathbf{z}} - \alpha \tilde{\mathbf{v}}) = (\tilde{\mathbf{v}}^\dagger \tilde{\mathbf{v}})^{-1} \tilde{\mathbf{v}}^\dagger \tilde{\mathbf{z}}$$

and

$$\begin{aligned}
\|\tilde{\mathbf{z}} - \alpha \tilde{\mathbf{v}}\|^2 &= \|\tilde{\mathbf{z}} - (\alpha - \alpha_1) \tilde{\mathbf{v}} - \alpha_1 \tilde{\mathbf{v}}\|^2 \\
&= \tilde{\mathbf{z}}^\dagger \mathbf{P}_{\tilde{\mathbf{v}}}^\perp \tilde{\mathbf{z}} + |\alpha - \alpha_1|^2 \tilde{\mathbf{v}}^\dagger \tilde{\mathbf{v}} \geq \tilde{\mathbf{z}}^\dagger \mathbf{P}_{\tilde{\mathbf{v}}}^\perp \tilde{\mathbf{z}} \quad (\text{A.18})
\end{aligned}$$

where $\tilde{\mathbf{z}} - \alpha_1 \tilde{\mathbf{v}} = \mathbf{P}_{\tilde{\mathbf{v}}}^\perp \tilde{\mathbf{z}}$. Thus, $\forall \alpha \geq \tilde{\mathbf{z}}^\dagger \mathbf{P}_{\tilde{\mathbf{v}}}^\perp \tilde{\mathbf{z}}$, the equation $(\tilde{\mathbf{z}} - \alpha \tilde{\mathbf{v}})^\dagger(\tilde{\mathbf{z}} - \alpha \tilde{\mathbf{v}}) = x$ is tantamount to $|\alpha - \alpha_1|^2 \tilde{\mathbf{v}}^\dagger \tilde{\mathbf{v}} = x - \tilde{\mathbf{z}}^\dagger \mathbf{P}_{\tilde{\mathbf{v}}}^\perp \tilde{\mathbf{z}}$ and is a circle centered at α_1 of proper radius. Similarly, l_2 attains its maximum at

$$\begin{aligned}
\alpha_2 &= \arg \min_{\alpha} \|\mathbf{P}_{\tilde{\mathbf{u}}}^\perp(\tilde{\mathbf{z}} - \alpha \tilde{\mathbf{v}})\|^2 \\
&= \arg \min_{\alpha} \|\mathbf{P}_{\tilde{\mathbf{u}}}^\perp \tilde{\mathbf{z}} - \alpha \mathbf{P}_{\tilde{\mathbf{u}}}^\perp \tilde{\mathbf{v}}\|^2 = (\tilde{\mathbf{v}}^\dagger \mathbf{P}_{\tilde{\mathbf{u}}}^\perp \tilde{\mathbf{v}})^{-1} \tilde{\mathbf{v}}^\dagger \mathbf{P}_{\tilde{\mathbf{u}}}^\perp \tilde{\mathbf{z}}
\end{aligned}$$

and

$$\begin{aligned}
\|\mathbf{P}_{\tilde{\mathbf{u}}}^\perp(\tilde{\mathbf{z}} - \alpha \tilde{\mathbf{v}})\|^2 &= \|\mathbf{P}_{\tilde{\mathbf{u}}}^\perp(\tilde{\mathbf{z}} - (\alpha - \alpha_2) \tilde{\mathbf{v}} - \alpha_2 \tilde{\mathbf{v}})\|^2 \\
&= \|\mathbf{P}_{\tilde{\mathbf{u}}}^\perp \tilde{\mathbf{z}} - \alpha_2 \mathbf{P}_{\tilde{\mathbf{u}}}^\perp \tilde{\mathbf{v}} - (\alpha - \alpha_2) \mathbf{P}_{\tilde{\mathbf{u}}}^\perp \tilde{\mathbf{v}}\|^2 \\
&= \left\| \left(\mathbf{I}_N - \mathbf{P}_{\tilde{\mathbf{u}}}^\perp \tilde{\mathbf{v}} (\tilde{\mathbf{v}}^\dagger \mathbf{P}_{\tilde{\mathbf{u}}}^\perp \tilde{\mathbf{v}})^{-1} \tilde{\mathbf{v}}^\dagger \mathbf{P}_{\tilde{\mathbf{u}}}^\perp \right) \right. \\
&\quad \times \left. \mathbf{P}_{\tilde{\mathbf{u}}}^\perp \tilde{\mathbf{z}} - (\alpha - \alpha_2) \mathbf{P}_{\tilde{\mathbf{u}}}^\perp \tilde{\mathbf{v}} \right\|^2 \\
&= \left\| \mathbf{P}_{\mathbf{P}_{\tilde{\mathbf{u}}}^\perp \tilde{\mathbf{v}}}^\perp \mathbf{P}_{\tilde{\mathbf{u}}}^\perp \tilde{\mathbf{z}} - (\alpha - \alpha_2) \mathbf{P}_{\tilde{\mathbf{u}}}^\perp \tilde{\mathbf{v}} \right\|^2 \\
&= \tilde{\mathbf{z}}^\dagger \mathbf{P}_{\tilde{\mathbf{u}}}^\perp \mathbf{P}_{\mathbf{P}_{\tilde{\mathbf{u}}}^\perp \tilde{\mathbf{v}}}^\perp \mathbf{P}_{\tilde{\mathbf{u}}}^\perp \tilde{\mathbf{z}} + |\alpha - \alpha_2|^2 \tilde{\mathbf{v}}^\dagger \mathbf{P}_{\tilde{\mathbf{u}}}^\perp \tilde{\mathbf{v}} \\
&= \tilde{\mathbf{z}}^\dagger \mathbf{P}_{\tilde{\mathbf{u}}}^\perp \tilde{\mathbf{z}} - \tilde{\mathbf{z}}^\dagger \mathbf{P}_{\tilde{\mathbf{u}}}^\perp \tilde{\mathbf{v}} (\tilde{\mathbf{v}}^\dagger \mathbf{P}_{\tilde{\mathbf{u}}}^\perp \tilde{\mathbf{v}})^{-1} \\
&\quad \times \tilde{\mathbf{v}}^\dagger \mathbf{P}_{\tilde{\mathbf{u}}}^\perp \tilde{\mathbf{z}} + |\alpha - \alpha_2|^2 \tilde{\mathbf{v}}^\dagger \mathbf{P}_{\tilde{\mathbf{u}}}^\perp \tilde{\mathbf{v}} \\
&\geq \tilde{\mathbf{z}}^\dagger \mathbf{P}_{\tilde{\mathbf{u}}}^\perp \tilde{\mathbf{z}} - \tilde{\mathbf{z}}^\dagger \mathbf{P}_{\tilde{\mathbf{u}}}^\perp \tilde{\mathbf{v}} (\tilde{\mathbf{v}}^\dagger \mathbf{P}_{\tilde{\mathbf{u}}}^\perp \tilde{\mathbf{v}})^{-1} \tilde{\mathbf{v}}^\dagger \mathbf{P}_{\tilde{\mathbf{u}}}^\perp \tilde{\mathbf{z}}. \quad (\text{A.19})
\end{aligned}$$

Thus, $\forall y \geq \tilde{\mathbf{z}}^\dagger \mathbf{P}_{\tilde{\mathbf{u}}}^\perp \tilde{\mathbf{z}} - \tilde{\mathbf{z}}^\dagger \mathbf{P}_{\tilde{\mathbf{u}}}^\perp \tilde{\mathbf{v}} (\tilde{\mathbf{v}}^\dagger \mathbf{P}_{\tilde{\mathbf{u}}}^\perp \tilde{\mathbf{v}})^{-1} \tilde{\mathbf{v}}^\dagger \mathbf{P}_{\tilde{\mathbf{u}}}^\perp \tilde{\mathbf{z}}$, the equation $\|\mathbf{P}_{\tilde{\mathbf{u}}}^\perp(\tilde{\mathbf{z}} - \alpha \tilde{\mathbf{v}})\|^2 = y$ is tantamount to

$|\alpha - \alpha_2|^2 \tilde{\mathbf{v}}^\dagger \mathbf{P}_{\tilde{\mathbf{u}}}^\perp \tilde{\mathbf{v}} = y - \tilde{\mathbf{z}}^\dagger \mathbf{P}_{\tilde{\mathbf{u}}}^\perp \tilde{\mathbf{z}} + \tilde{\mathbf{z}}^\dagger \mathbf{P}_{\tilde{\mathbf{u}}}^\perp \tilde{\mathbf{v}} (\tilde{\mathbf{v}}^\dagger \mathbf{P}_{\tilde{\mathbf{u}}}^\perp \tilde{\mathbf{v}})^{-1} \tilde{\mathbf{v}}^\dagger \mathbf{P}_{\tilde{\mathbf{u}}}^\perp \tilde{\mathbf{z}}$ and is a circle centered at α_2 of proper radius.

Obviously, for $\alpha_1 = \alpha_2$ the maximum of $l(b, \alpha)$, given b , is attained at α_1 . Assuming instead $\alpha_1 \neq \alpha_2$, we can prove that the values of α maximizing $l(b, \alpha)$ belong to the segment whose endpoints are α_1 and α_2 , indicated hereafter as $\mathcal{S}_{\alpha_1 \alpha_2}$.

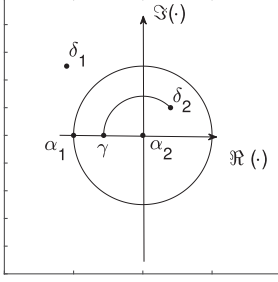


Fig. 7. Illustration of the procedure to find points of the “segment $\alpha_1 - \alpha_2$ ” that upperbound $l(b, \alpha)$. Without loss of generality $\alpha_2 = 0$ and $\alpha_1 < 0$.

To this end, we show that $\forall \alpha \in \mathbb{C} \setminus \mathcal{S}_{\alpha_1 \alpha_2}$ there exists a point $\bar{\alpha} \in \mathcal{S}_{\alpha_1 \alpha_2}$ such that

$$l(b, \alpha) < l(b, \bar{\alpha}). \quad (\text{A.20})$$

In fact, if $\alpha \in \mathbb{C}$ does not belong to the circle centered at α_2 of radius $|\alpha_1 - \alpha_2|$ as, for instance, δ_1 in Fig. 7, we can choose $\bar{\alpha} = \alpha_1$ that has a smaller distance from α_2 than δ_1 , thus implying $\|\mathbf{P}_{\tilde{\mathbf{u}}}^\perp(\tilde{\mathbf{z}} - \delta_1 \tilde{\mathbf{v}})\|^2 > \|\mathbf{P}_{\tilde{\mathbf{u}}}^\perp(\tilde{\mathbf{z}} - \alpha_1 \tilde{\mathbf{v}})\|^2$, $\|\tilde{\mathbf{z}} - \delta_1 \tilde{\mathbf{v}}\|^2 > \|\tilde{\mathbf{z}} - \alpha_1 \tilde{\mathbf{v}}\|^2$ and, eventually $l(b, \delta_1) < l(b, \alpha_1)$.

If, instead, $\alpha \in \mathbb{C} \setminus \mathcal{S}_{\alpha_1 \alpha_2}$ belongs to the circle centered at α_2 of radius $|\alpha_1 - \alpha_2|$ as, for instance, δ_2 in Fig. 7, we replace it with γ , i.e., $\bar{\alpha} = \gamma$, that has the same distance of δ_2 from α_2 and a smaller distance from α_1 , thus implying $\|\mathbf{P}_{\tilde{\mathbf{u}}}^\perp(\tilde{\mathbf{z}} - \delta_2 \tilde{\mathbf{v}})\|^2 = \|\mathbf{P}_{\tilde{\mathbf{u}}}^\perp(\tilde{\mathbf{z}} - \gamma \tilde{\mathbf{v}})\|^2$, $\|\tilde{\mathbf{z}} - \delta_2 \tilde{\mathbf{v}}\|^2 > \|\tilde{\mathbf{z}} - \gamma \tilde{\mathbf{v}}\|^2$ and, eventually $l(b, \delta_2) < l(b, \gamma)$.

APPENDIX B PROOF OF PROPOSITION 3

The derivative of $f(\nu)$ is given by

$$\begin{aligned} \frac{d}{d\nu} f(\nu) &= \frac{N}{K+1} (1+\nu)^{\frac{N}{K+1}-1} \left(1 + \frac{a}{1+\nu}\right) \\ &\quad - (1+\nu)^{\frac{N}{K+1}} \frac{a}{(1+\nu)^2}. \end{aligned}$$

Thus, $\frac{d}{d\nu} f(\nu) < 0$ if and only if $\frac{N}{K+1}(1+\nu+a) - a < 0$ or, equivalently, $\nu < (\frac{K+1}{N} - 1)a - 1$. It follows that the function $f(\nu)$ attains its minimum over $[0, +\infty)$ at $\hat{\nu} = (\frac{K+1}{N} - 1)a - 1$ if such a value is positive and at 0 otherwise.

CHARACTERIZATION OF DETECTORS (12) AND (15).

First we compute the P_{fa} of the parametric detector (15) and, as a special case, that of the GLRT (12). To this end, let

$$\tilde{t}_K = \frac{t_K}{1-t_K} = \frac{\frac{|z^\dagger \mathbf{S}^{-1} \mathbf{v}|^2}{\mathbf{v}^\dagger \mathbf{S}^{-1} \mathbf{v}}}{1 + z^\dagger \mathbf{S}^{-1} \mathbf{z} - \frac{|z^\dagger \mathbf{S}^{-1} \mathbf{v}|^2}{\mathbf{v}^\dagger \mathbf{S}^{-1} \mathbf{v}}} \quad (\text{B.21})$$

where $t_K = \frac{|z^\dagger \mathbf{S}^{-1} \mathbf{v}|^2}{\mathbf{v}^\dagger \mathbf{S}^{-1} \mathbf{v}(1+z^\dagger \mathbf{S}^{-1} \mathbf{z})}$ is Kelly’s statistic and

$$b = \frac{1}{1 + z^\dagger \mathbf{S}^{-1} \mathbf{z} - \frac{|z^\dagger \mathbf{S}^{-1} \mathbf{v}|^2}{\mathbf{v}^\dagger \mathbf{S}^{-1} \mathbf{v}}}. \quad (\text{B.22})$$

It turns out that $1 + \|\tilde{\mathbf{z}}\|^2 = 1 + z^\dagger \mathbf{S}^{-1} \mathbf{z} = (1 + \tilde{t}_K) / b$ and $\|\mathbf{P}_{\tilde{\mathbf{v}}}^\perp \tilde{\mathbf{z}}\|^2 = z^\dagger \mathbf{S}^{-1} \mathbf{z} - \frac{|z^\dagger \mathbf{S}^{-1} \mathbf{v}|^2}{\mathbf{v}^\dagger \mathbf{S}^{-1} \mathbf{v}} = \frac{1}{b} - 1$ and, hence, the decision statistic of the detector (15) can be re-written as

$$\Lambda_\epsilon(\mathbf{z}, \mathbf{S}) = \begin{cases} \frac{\frac{1+\tilde{t}_K}{b} \left(1 - \frac{1}{\zeta_\epsilon}\right)}{\left[(\zeta_\epsilon - 1) \left(\frac{1}{b} - 1\right)\right]^{\frac{1}{\zeta_\epsilon}}}, & b < 1 - \frac{1}{\zeta_\epsilon} \\ 1 + \tilde{t}_K, & \text{otherwise.} \end{cases} \quad (\text{B.23})$$

Under the noise-only hypothesis the random variable (RV) \tilde{t}_K , given by equation (B.21), is distributed according to a complex central F-distribution with 1 and $K - N + 1$ (complex) degrees of freedom and it is independent of b , given by equation (B.22), which, in turn, obeys a complex central beta distribution with $K - N + 2$ and $N - 1$ (complex) degrees of freedom [3], [26], [27]. In symbols, we write $\tilde{t}_K \sim \mathcal{CF}_{1, K-N+1}$ and $b \sim \mathcal{CB}_{K-N+2, N-1}$. It is thus apparent that P_{fa} is independent of \mathbf{C} and, hence, the detector possesses the CFAR property.

Moreover, we can compute P_{fa} as follows

$$P_{fa} = \int_0^1 \mathbf{P}[\Lambda_\epsilon(\mathbf{z}, \mathbf{S}) > \eta | b = x, H_0] f_b(x) dx$$

where $f_b(\cdot)$ denotes the PDF of the RV b [27], i.e.,

$$f_b(x) = \frac{1}{B(K+2-N, N-1)} x^{K-N+1} (1-x)^{N-2}$$

with $0 \leq x \leq 1$, while

$$\begin{aligned} p(x) &= \mathbf{P}[\Lambda_\epsilon(\mathbf{z}, \mathbf{S}) > \eta | b = x, H_0] \\ &= \begin{cases} 1 - F_{\tilde{t}_K}^-(y_\epsilon(x)), & 0 \leq x \leq 1 - \frac{1}{\zeta_\epsilon} \\ 1 - F_{\tilde{t}_K}^-(\eta - 1), & 1 - \frac{1}{\zeta_\epsilon} \leq x \leq 1 \end{cases} \end{aligned}$$

with [27, formula (A.7)]

$$1 - F_{\tilde{t}_K}^-(y_\epsilon) = \begin{cases} \frac{1}{(1+y_\epsilon)^{K-N+1}}, & y_\epsilon \geq 0 \\ 1, & y_\epsilon < 0 \end{cases}$$

and $y_\epsilon(x) = \eta x \left((\zeta_\epsilon - 1) \frac{1-x}{x} \right)^{\frac{1}{\zeta_\epsilon}} \frac{\zeta_\epsilon}{\zeta_\epsilon - 1} - 1$. To compute the P_{fa} , we observe that the derivative of $y_\epsilon(x)$ is given by

$$\frac{dy_\epsilon(x)}{dx} = \eta \left((\zeta_\epsilon - 1) \frac{1-x}{x} \right)^{\frac{1}{\zeta_\epsilon}-1} \left(\zeta_\epsilon \frac{1-x}{x} - \frac{1}{x} \right)$$

and it is positive for $0 < x < 1 - \frac{1}{\zeta_\epsilon}$. Moreover, $\lim_{x \rightarrow 0^+} y_\epsilon(x) = -1$ and $y_\epsilon(1 - \frac{1}{\zeta_\epsilon}) = \eta - 1$. It turns out that $P_{fa} = 1$ for $\eta \leq 1$. If, instead, $\eta > 1$, denoting by $\bar{x}_\epsilon(\eta)$ that number in $(0, 1 - \frac{1}{\zeta_\epsilon})$ such that $y_\epsilon(\bar{x}_\epsilon) = 0$, it follows that

$$\begin{aligned} P_{fa} &= \int_0^{\bar{x}_\epsilon(\eta)} f_b(x) dx + \int_{\bar{x}_\epsilon(\eta)}^{1 - \frac{1}{\zeta_\epsilon}} \frac{1}{[1 + y_\epsilon(x)]^{K+1-N}} f_b(x) dx \\ &\quad + \frac{1}{\eta^{K+1-N}} \int_{1 - \frac{1}{\zeta_\epsilon}}^1 f_b(x) dx \end{aligned}$$

i.e., introducing $c = \frac{1}{B(K+2-N, N-1)} = \frac{K!}{(K+1-N)!(N-2)!}$,

$$P_{fa} = c \int_0^{\bar{x}_\epsilon(\eta)} x^{K-N+1} (1-x)^{N-2} dx$$

$$+ \frac{a_\epsilon c}{\eta^{K+1-N}} \int_{\bar{x}_\epsilon(\eta)}^{1-\frac{1}{\zeta_\epsilon}} x^{\frac{K+1-N}{\zeta_\epsilon}} (1-x)^{N-2-\frac{K+1-N}{\zeta_\epsilon}} dx$$

$$+ \frac{c}{\eta^{K+1-N}} \int_{1-\frac{1}{\zeta_\epsilon}}^1 x^{K-N+1} (1-x)^{N-2} dx$$

where $a_\epsilon = \frac{(\frac{\zeta_\epsilon-1}{\zeta_\epsilon})^{K+1-N}}{(\frac{\zeta_\epsilon-1}{\zeta_\epsilon})^{\frac{K+1-N}{\zeta_\epsilon}}}$. The P_{fa} of (15) is thus given by

$$P_{fa} = cB_{\bar{x}_\epsilon(\eta)}(K-N+2, N-1) + \frac{a_\epsilon c}{\eta^{K+1-N}}$$

$$\times \left[B_{1-\frac{1}{\zeta_\epsilon}} \left(\frac{K+1-N}{\zeta_\epsilon} + 1, N-1 - \frac{K+1-N}{\zeta_\epsilon} \right) \right.$$

$$\left. - B_{\bar{x}_\epsilon(\eta)} \left(\frac{K+1-N}{\zeta_\epsilon} + 1, N-1 - \frac{K+1-N}{\zeta_\epsilon} \right) \right]$$

$$+ \frac{c}{\eta^{K+1-N}} \left[B(K-N+2, N-1) \right.$$

$$\left. - B_{1-\frac{1}{\zeta_\epsilon}}(K-N+2, N-1) \right] \quad (\text{B.24})$$

where $B(\cdot, \cdot)$ is the Eulerian beta function while $B_u(\nu, \mu) = \int_0^u t^{\nu-1} (1-t)^{\mu-1} dt$ is the incomplete beta function [28].

As a special case, i.e., $\epsilon = 0$ and, hence, $\zeta_\epsilon = \zeta$, we obtain the P_{fa} of the GLRT (12).

On the other hand, if we suppose that under the H_1 hypothesis the actual useful signal is deterministic, but with a steering vector \mathbf{p} different from the nominal one \mathbf{v} , i.e.,

$$\mathbf{r} = \alpha \mathbf{p} + \mathbf{n}, \quad \mathbf{n} \sim \mathcal{CN}_N(\mathbf{0}, \mathbf{C}),$$

\tilde{t}_K , given b , is ruled by a complex noncentral F-distribution with 1 and $K-N+1$ (complex) degrees of freedom and noncentrality parameter δ , with [4], [27], [29]

$$\delta^2 = \text{SNR} \cdot b \cos^2 \theta,$$

where

$$\text{SNR} = |\alpha|^2 \mathbf{p}^\dagger \mathbf{C}^{-1} \mathbf{p} \quad (\text{B.25})$$

and

$$\cos^2 \theta = \frac{|\mathbf{p}^\dagger \mathbf{C}^{-1} \mathbf{v}|^2}{(\mathbf{v}^\dagger \mathbf{C}^{-1} \mathbf{v})(\mathbf{p}^\dagger \mathbf{C}^{-1} \mathbf{p})}. \quad (\text{B.26})$$

In addition, the RV b obeys the complex noncentral beta distribution with $K-N+2$ and $N-1$ (complex) degrees of freedom and noncentrality parameter δ_b , with

$$\delta_b^2 = \text{SNR} \cdot \sin^2 \theta.$$

In symbols, we write $\tilde{t}_K \sim \mathcal{CF}_{1, K-N+1}(\delta)$ and $b \sim \mathcal{CB}_{K-N+2, N-1}(\delta_b)$.

In the special case of perfect match between \mathbf{p} and \mathbf{v} , then $\delta^2 = |\alpha|^2 \mathbf{v}^\dagger \mathbf{C}^{-1} \mathbf{v} \cdot b$ and $\delta_b^2 = 0$, i.e., $b \sim \mathcal{CB}_{K-N+2, N-1}$ and $\tilde{t}_K \sim \mathcal{CF}_{1, K-N+1}(\delta)$ given b .

The above characterization highlights that performance of detectors (12) and (15) can be expressed in terms of P_d vs SNR (equation (B.25)) given $\cos^2 \theta$ (equation (B.26)) and P_{fa} . In principle, such characterization could be exploited to compute P_d , paralleling the computation of P_{fa} ; however, analytical forms for P_d are less useful since Monte Carlo simulation is not very time-consuming. As a matter of fact, we use Monte Carlo simulation to compute P_d vs SNR, expressed by equation (B.25), given $\cos^2 \theta$ and P_{fa} .

We focus on the binary hypotheses testing problem

$$\begin{cases} H_0 : \mathbf{z} \sim \mathcal{CN}_N(\mathbf{0}, \mathbf{C}) \\ H_1 : \mathbf{z} \sim \mathcal{CN}_N(\alpha \mathbf{v}, \nu \mathbf{u} \mathbf{u}^\dagger + \mathbf{C}) \end{cases}$$

where $\nu \geq 0$ and $\alpha \in \mathbb{C}$ are unknown quantities while the vectors $\mathbf{u}, \mathbf{v} \in \mathbb{C}^{N \times 1}$ and the Hermitian positive definite matrix \mathbf{C} are known. The corresponding GLRT is given by

$$\Lambda(\mathbf{z}, \mathbf{C}) = \frac{\max_{\nu \geq 0} \max_{\alpha \in \mathbb{C}} f_1(\mathbf{z}|\nu, \alpha)}{f_0(\mathbf{z})} \underset{H_0}{\overset{H_1}{>}} \eta \quad (\text{C.27})$$

where

$$f_1(\mathbf{z}|\nu, \alpha) = \frac{1}{\pi^N} \frac{1}{(1 + \nu \mathbf{u}^\dagger \mathbf{C}^{-1} \mathbf{u}) \det(\mathbf{C})} l(\nu, \alpha)$$

is the PDF of \mathbf{z} under H_1 with

$$l(\nu, \alpha) = e^{-\mathbf{z}^\dagger \mathbf{C}^{-1} \mathbf{z} + \nu \frac{|\mathbf{u}^\dagger \mathbf{C}^{-1} (\mathbf{z} - \alpha \mathbf{v})|^2}{1 + \nu \mathbf{u}^\dagger \mathbf{C}^{-1} \mathbf{u}}}$$

while $f_0(\mathbf{z})$, the PDF of \mathbf{z} under H_0 , is given by

$$f_0(\mathbf{z}) = \frac{1}{\pi^N \det(\mathbf{C})} e^{-\mathbf{z}^\dagger \mathbf{C}^{-1} \mathbf{z}}.$$

To maximize $l(\nu, \alpha)$ over α we rewrite its exponent as

$$-\mathbf{z}^\dagger \mathbf{C}^{-1} \mathbf{z} + \nu \frac{|\mathbf{u}^\dagger \mathbf{C}^{-1} (\mathbf{z} - \alpha \mathbf{v})|^2}{1 + \nu \mathbf{u}^\dagger \mathbf{C}^{-1} \mathbf{u}}$$

$$= -\|\tilde{\mathbf{z}} - \alpha \tilde{\mathbf{v}}\|^2 + \nu \frac{|\tilde{\mathbf{u}}^\dagger (\tilde{\mathbf{z}} - \alpha \tilde{\mathbf{v}})|^2}{1 + \nu \|\tilde{\mathbf{u}}\|^2}$$

where $\tilde{\mathbf{z}} = \mathbf{C}^{-1/2} \mathbf{z}$, $\tilde{\mathbf{v}} = \mathbf{C}^{-1/2} \mathbf{v}$, and $\tilde{\mathbf{u}} = \mathbf{C}^{-1/2} \mathbf{u}$. Using

$$\|\tilde{\mathbf{z}} - \alpha \tilde{\mathbf{v}}\|^2 = \|\mathbf{P}_{\tilde{\mathbf{u}}} (\tilde{\mathbf{z}} - \alpha \tilde{\mathbf{v}})\|^2 + \|\mathbf{P}_{\tilde{\mathbf{u}}}^\perp (\tilde{\mathbf{z}} - \alpha \tilde{\mathbf{v}})\|^2$$

and

$$|\tilde{\mathbf{u}}^\dagger (\tilde{\mathbf{z}} - \alpha \tilde{\mathbf{v}})|^2 = \|\tilde{\mathbf{u}}\|^2 \|\mathbf{P}_{\tilde{\mathbf{u}}} (\tilde{\mathbf{z}} - \alpha \tilde{\mathbf{v}})\|^2$$

we obtain

$$l(\nu, \alpha) = e^{-\frac{\|\tilde{\mathbf{z}} - \alpha \tilde{\mathbf{v}}\|^2 + \nu \|\tilde{\mathbf{u}}\|^2 \|\mathbf{P}_{\tilde{\mathbf{u}}}^\perp (\tilde{\mathbf{z}} - \alpha \tilde{\mathbf{v}})\|^2}{1 + \nu \|\tilde{\mathbf{u}}\|^2}}.$$

Now letting $\mathbf{u} = \mathbf{v}$ and, hence, $\tilde{\mathbf{u}} = \tilde{\mathbf{v}}$ we have an expression that can be easily maximized with respect to α obtaining

$$\max_{\alpha \in \mathbb{C}} l(\nu, \alpha) = e^{-\|\mathbf{P}_{\tilde{\mathbf{v}}}^\perp \tilde{\mathbf{z}}\|^2}$$

and hence

$$\max_{\alpha \in \mathbb{C}} f_1(\mathbf{z}|\nu, \alpha) = \frac{1}{\pi^N} \frac{1}{(1 + \nu \mathbf{v}^\dagger \mathbf{C}^{-1} \mathbf{v}) \det(\mathbf{C})} e^{-\|\mathbf{P}_{\tilde{\mathbf{v}}}^\perp \tilde{\mathbf{z}}\|^2}.$$

It follows that

$$\max_{\nu \geq 0} \max_{\alpha \in \mathbb{C}} f_1(\mathbf{z}|\nu, \alpha) = \frac{1}{\pi^N} \frac{1}{\det(\mathbf{C})} e^{-\|\mathbf{P}_{\tilde{\mathbf{v}}}^\perp \tilde{\mathbf{z}}\|^2}$$

and

$$\Lambda(\mathbf{z}, \mathbf{C}) = e^{\|\mathbf{P}_{\tilde{\mathbf{v}}} \tilde{\mathbf{z}}\|^2} = e^{\frac{|\mathbf{z}^\dagger \mathbf{C}^{-1} \mathbf{v}|^2}{\mathbf{v}^\dagger \mathbf{C}^{-1} \mathbf{v}}} \underset{H_0}{\overset{H_1}{>}} \eta. \quad (\text{C.28})$$

The corresponding adaptive detector, obtained by replacing C with the sample covariance matrix based on the secondary data, is obviously equivalent to the AMF.

REFERENCES

- [1] J. Ward, "Space-time adaptive processing for airborne radar," MIT Lincoln Lab., Lexington, MA, USA, Tech. Rep. 1015, Dec. 1994.
- [2] R. Klemm, *Principles of Space-Time Adaptive Processing* (IEE Radar, Sonar, Navigation and Avionics Series 12). London, U.K.: The Institute of Electrical Engineers, 2002.
- [3] E. J. Kelly, "An adaptive detection algorithm," *IEEE Trans. Aerosp. Electron. Syst.*, vol. 22, no. 2, pp. 115–127, Mar. 1986.
- [4] E. J. Kelly, "Performance of an adaptive detection algorithm; rejection of unwanted signals," *IEEE Trans. Aerosp. Electron. Syst.*, vol. 25, no. 2, pp. 122–133, Mar. 1989.
- [5] F. C. Robey, D. L. Fuhrman, E. J. Kelly, and R. Nitzberg, "A CFAR adaptive matched filter detector," *IEEE Trans. Aerosp. Electron. Syst.*, vol. 29, no. 1, pp. 208–216, Jan. 1992.
- [6] S. Kraut and L. L. Scharf, "The CFAR adaptive subspace detector is a scale-invariant GLRT," *IEEE Trans. Signal Process.*, vol. 47, no. 9, pp. 2538–2541, Sep. 1999.
- [7] N. B. Pulsone and C. M. Rader, "Adaptive beamformer orthogonal rejection test," *IEEE Trans. Signal Process.*, vol. 49, no. 3, pp. 521–529, Mar. 2001.
- [8] G. A. Fabrizio, A. Farina, and M. D. Turley, "Spatial adaptive subspace detection in OTH radar," *IEEE Trans. Aerosp. Electron. Syst.*, vol. 39, no. 4, pp. 1407–1427, Oct. 2003.
- [9] F. Bandiera, O. Besson, and G. Ricci, "An ABORT-like detector with improved mismatched signals rejection capabilities," *IEEE Trans. Signal Process.*, vol. 56, no. 1, pp. 14–25, Jan. 2008.
- [10] S. Z. Kalson, "An adaptive array detector with mismatched signal rejection," *IEEE Trans. Aerosp. Electron. Syst.*, vol. 28, no. 1, pp. 195–207, Jan. 1992.
- [11] F. Bandiera, D. Orlando, and G. Ricci, "One- and two-stage tunable receivers*," *IEEE Trans. Signal Process.*, vol. 57, no. 8, pp. 3264–3273, Aug. 2009.
- [12] J. Liu, S. Zhou, W. Liu, J. Zheng, H. Liu, and J. Li, "Tunable adaptive detection in colocated MIMO radar," *IEEE Trans. Signal Process.*, vol. 66, no. 4, pp. 1080–1092, Feb. 15, 2018.
- [13] J. Liu, H.-Y. Zhao, W. Liu, H. Li, and H. Liu, "Adaptive detection using both the test and training data for disturbance correlation estimation," *Signal Process.*, vol. 137, pp. 309–318, 2017.
- [14] A. De Maio, "Robust adaptive radar detection in the presence of steering vector mismatches," *IEEE Trans. Aerosp. Electron. Syst.*, vol. 41, no. 4, pp. 1322–1337, Oct. 2005.
- [15] O. Besson, "Detection of a signal in linear subspace with bounded mismatch," *IEEE Trans. Aerosp. Electron. Syst.*, vol. 42, no. 3, pp. 1131–1139, Jul. 2006.
- [16] C. Hao, B. Liu, and L. Cai, "Performance analysis of a two-stage Rao detector," *Signal Process.*, vol. 91, pp. 2141–2146, 2011.
- [17] J. Liu, W. Liu, B. Chen, H. Liu, H. Li, and C. Hao, "Modified Rao test for multichannel adaptive signal detection," *IEEE Trans. Signal Process.*, vol. 64, no. 3, pp. 714–725, Feb. 1, 2016.
- [18] J. Liu, K. Li, X. Zhang, M. Liu, and W. Liu, "A weighted detector for mismatched subspace signals," *Signal Process.*, vol. 140, pp. 110–115, 2017.
- [19] K. Duan, M. Liu, H. Dai, F. Xu, and W. Liu, "A two-stage detector for mismatched subspace signals," *IEEE Geosci. Remote Sens. Lett.*, vol. 14, no. 12, pp. 2270–2274, Dec. 2017.
- [20] D. Ciuonzo, A. De Maio, and D. Orlando, "A unifying framework for adaptive radar detection in homogeneous plus structured interference—Part II: Detectors design," *IEEE Trans. Signal Process.*, vol. 64, no. 11, pp. 2907–2919, Jun. 1, 2016.
- [21] D. Ciuonzo, A. De Maio, and D. Orlando, "On the statistical invariance for adaptive radar detection in partially homogeneous disturbance plus structured interference," *IEEE Trans. Signal Process.*, vol. 65, no. 5, pp. 1222–1234, Mar. 1, 2017.
- [22] O. Besson, E. Chaumette, and F. Vincent, "Adaptive detection of a Gaussian signal in Gaussian noise," in *Proc. 6th IEEE Int. Workshop Comput. Adv. Multi-Sensor Adaptive Process.*, Cancún, Mexico, Dec. 2015, pp. 117–120.
- [23] O. Besson, A. Coluccia, E. Chaumette, G. Ricci, and F. Vincent, "Generalized likelihood ratio test for detection of Gaussian rank-one signals in Gaussian noise with unknown statistics," *IEEE Trans. Signal Process.*, vol. 65, no. 4, pp. 1082–1092, Feb. 15, 2017.

- [24] A. Coluccia and G. Ricci, "A random-signal approach to robust radar detection," in *Proc. 52nd Annu. Conf. Inf. Sci. Syst.*, Princeton, NJ, USA, Mar. 2018, pp. 1–6.
- [25] R. A. Horn and C. R. Johnson, *Matrix Analysis*. Cambridge, U.K.: Cambridge Univ. Press, 1985.
- [26] E. J. Kelly and K. Forsythe, "Adaptive detection and parameter estimation for multidimensional signal models," MIT Lincoln Lab., Lexington, MA, USA, Tech. Rep. 848, Apr. 19, 1989.
- [27] F. Bandiera, D. Orlando, and G. Ricci, "Advanced radar detection schemes under mismatched signal models," in *Synthesis Lectures on Signal Processing No. 8*. San Rafael, CA, USA: Morgan & Claypool, 2009.
- [28] L. S. Gradshteyn and I. M. Ryzhik, *Table of Integrals, Series, and Products*, 6th ed. New York, NY, USA: Academic, 2000.
- [29] E. J. Kelly, "Adaptive detection in non-stationary interference—Part III," MIT Lincoln Lab., Lexington, MA, USA, Tech. Rep. 761, Aug. 1987.
- [30] A. Coluccia, A. Fascista, and G. Ricci, "A novel approach to robust radar detection of range-spread targets," *Signal Process.*, vol. 166, Jan. 2019, Art. no. 107223. [Online]. Available: <https://doi.org/10.1016/j.sigpro.2019.07.016>



Angelo Coluccia (M'13–SM'16) received the Eng. degree in telecommunication engineering (*summa cum laude*) and the Ph.D. degree in information engineering from the University of Salento, Lecce, Italy, in 2007 and 2011, respectively. He is completing a tenure-track for Associate Professor with the Dipartimento di Ingegneria dell'Innovazione, University of Salento, where he teaches Telecommunication Systems. Since 2008, he has been engaged in European research projects on different topics, including small-drone detection, tracking, and data fusion. He

has been a Researcher with Forschungszentrum Telekommunikation Wien, Vienna, Austria, working on mobile Internet traffic modeling and anomaly detection. He has held a visiting position with the Department of Electronics, Optronics, and Signals (DEOS) of the Institut Supérieur de l'Aéronautique et de l'Espace, ISAE-Supaéro, Toulouse, France, in the Signal, Communication, Antennas and Navigation (SCAN) Group. His research interests are multi-sensor and multi-agent statistical signal processing for detection, estimation, learning, and localization problems. Relevant application fields are radar, wireless networks (including 5G), intelligent cyber-physical systems, and emerging network contexts (including smart devices and social networks). He is a Member of the Special Area Team in Signal Processing for Multisensor Systems of EURASIP.



Giuseppe Ricci (M'01–SM'10) was born in Naples, Italy, on February 15, 1964. He received the Dr. and Ph.D. degrees in electronic engineering from the University of Naples "Federico II," Naples, Italy, in 1990 and 1994, respectively. Since 1995, he has been with the University of Salento (formerly University of Lecce), Lecce, Italy, first as an Assistant Professor of Telecommunications and, since 2002, as a Professor. His research interests are in the field of statistical signal processing with emphasis on radar processing, localization algorithms, and CDMA systems. More

precisely, he has focused on high-resolution radar clutter modeling, detection of radar signals in Gaussian and non-Gaussian disturbance, oil spill detection from SAR data, track-before-detect algorithms fed by space-time radar data, localization in wireless sensor networks, multiuser detection in overlay CDMA systems, and blind multiuser detection. He has held visiting positions with the University of Colorado, Boulder, CO, USA, from 1997 to 1998 and in April/May 2001, with the Colorado State University, Fort Collins, CO, USA, in July/September 2003, March 2005, September 2009, and March 2011, with Ensica, Toulouse, France, in March 2006, and with the University of Connecticut, Storrs, CT, USA, in September 2008.



Olivier Besson received the Ph.D. degree in signal processing from Institut National Polytechnique Toulouse, Toulouse, France, in 1992. He is currently a Professor with Institut Supérieur de l'Aéronautique et de l'Espace (ISAE-SUPAÉRO), Toulouse, France. His research interests are in statistical array processing, multivariate analysis, adaptive detection, and estimation.